Senior Thesis

A STRUCTURAL ANALYSIS OF THE 'S'-FOLD IN ROCK CANYON, GUNNISON PLATEAU, CENTRAL UTAH

by
Douglas S. Kilmer
1988

Submitted as a partial fulfillment of
the requirements for the degree of
Bachelor of Science in Geology and
Mineralogy at The Ohio State University,
Spring Quarter, 1988

Approved by:

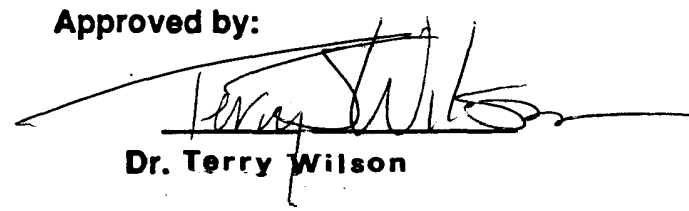

Dr. Terry Wilson

RESEARCH AWARD

1988

ACKNOWLEDGEMENTS

I would like to take this chance to thank all of the people who helped me to secure this ticket to freedom; my parents for paying the endless flow of bills; my brother-in-law Doug Liberati for the formatting and graphics for this paper; Drs. Marcia Bjornerud, William Ausich, 'and Peter Schwans for assistance in their specific fields; and to my advisor, Dr. Terry Wilson, for leading me through the dark and putting up with my constant annoying presence.

A STRUCTURAL ANALYSIS OF THE "S"-FOLD IN ROCK CANYON, GUNNISON PLATEAU, CENTRAL UTAH

INTRODUCTION

The Gunnison Plateau is in the transition zone in Central Utah between the Colorado Plateau and Basin and Range geomorphic provinces. The region has been affected by folding and thrusting of the Sevier orogenic belt, and then later by normal faulting associated with crustal extension of the Basin and Range Province. A major asymmetric flexure, termed in this paper the "S"-fold, runs along the eastern flank of the Gunnison Plateau (e.g. Weiss, 1982). The site for the present study of this "S"-fold was the mouth of Rock Canyon, located approximately 5.5km due west of Ephraim, Utah, within the Manti Quadrangle (see Figure 1).

The"S"-fold, seen looking north from the south side of Dry Canyon, approximately 500m south of the study area, is shown in Figure 2a. Figure 2b is a tracing of the photograph that shows the bedding contacts and the structure of the fold. The purpose of this study was to evaluate mechanics proposed for the origin of this structure based on meso- and microscopic examinations of stylolites and calcite veins present at this location.

AFFECTED UNITS

The stratigraphic succession in this part of Central Utah is shown in the column in Figure 3. The units that are contained in the "S"-fold in Rock Canyon are the Late Paleocne-Early Eocene Flagstaff Formation and the Late Cretaceous-Early Tertiary North Horn Formation. To the north units of an older age are incorporated into the fold. The Flagstaff Formation is a massive lacustrine limestone containing gastropods, bivalves, and oncolites. The North Horn is made up of a mixture of shales, fluvial sandstones, and a basal conglomerate, and rapidly changes facies laterally.

The North Horn Formation rests with angular unconformity on the Twist Gulch Member of the Arapien Shale Formation. The Twist Gulch occupies the core of the "S"-fold. It is formed from interlayered chocolate - colored silt - and sandstones. The Arapien is a shale with interspersed evaporites.

Overlying the Flagstaff Formation are the Middle Tertiary Colton and Green River Formations. It could not be determined in the field whether these units were originally part of the fold or not because they are missing at the site due to erosion. However, half a kilometer to the west on the plateau these units are lying conformably on the Flagstaff, indicating there is a possibility the units were part of the fold.

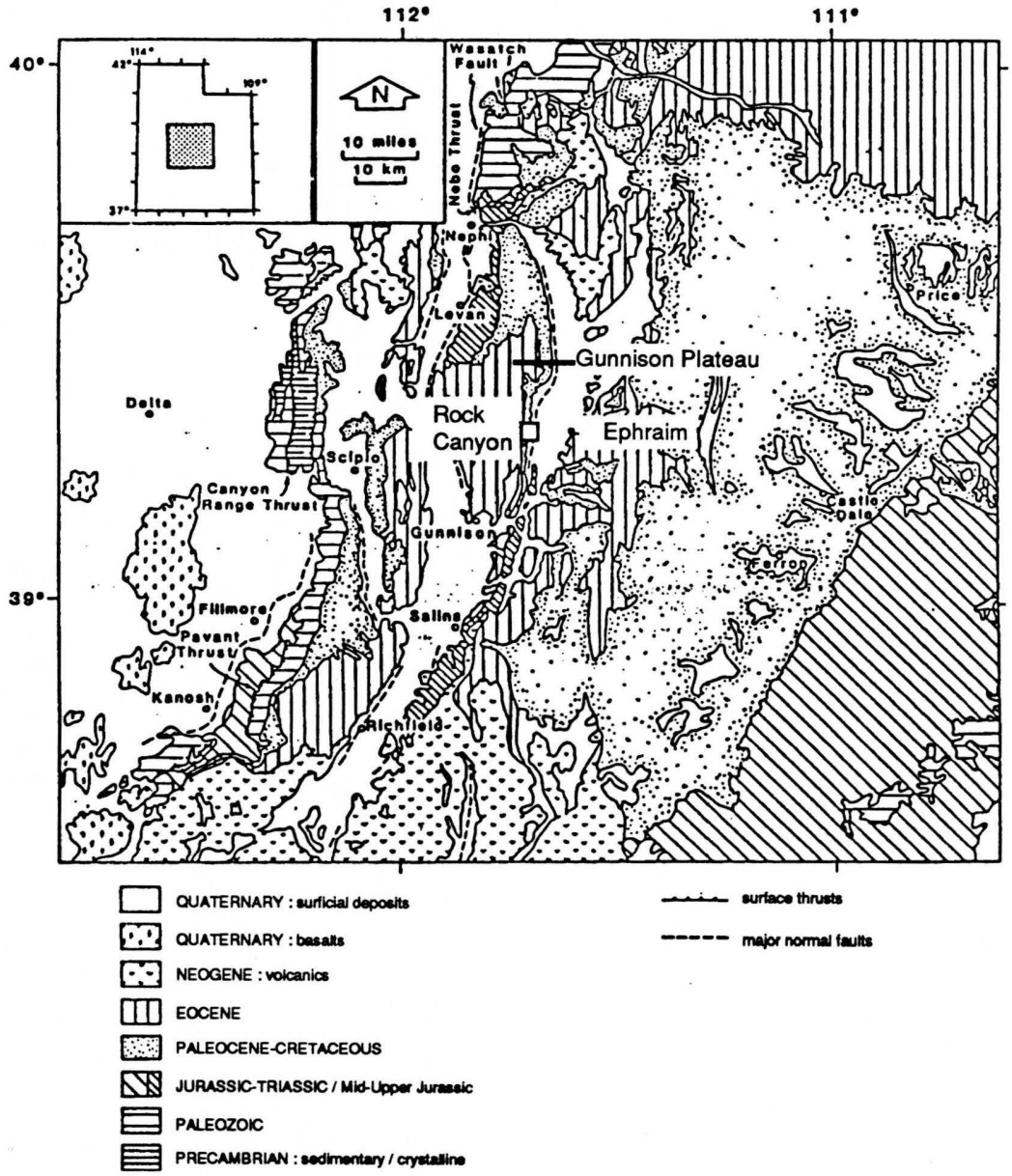

Figure 1. Map of the Gunnison Plateau and the surrounding localities of the Central Utah (Modified from Villien and Kligfield, 1986).

Figure 2a. Photograph of the "S"-Fold in Dry Canyon. View is looking north from the south wall of the canyon.

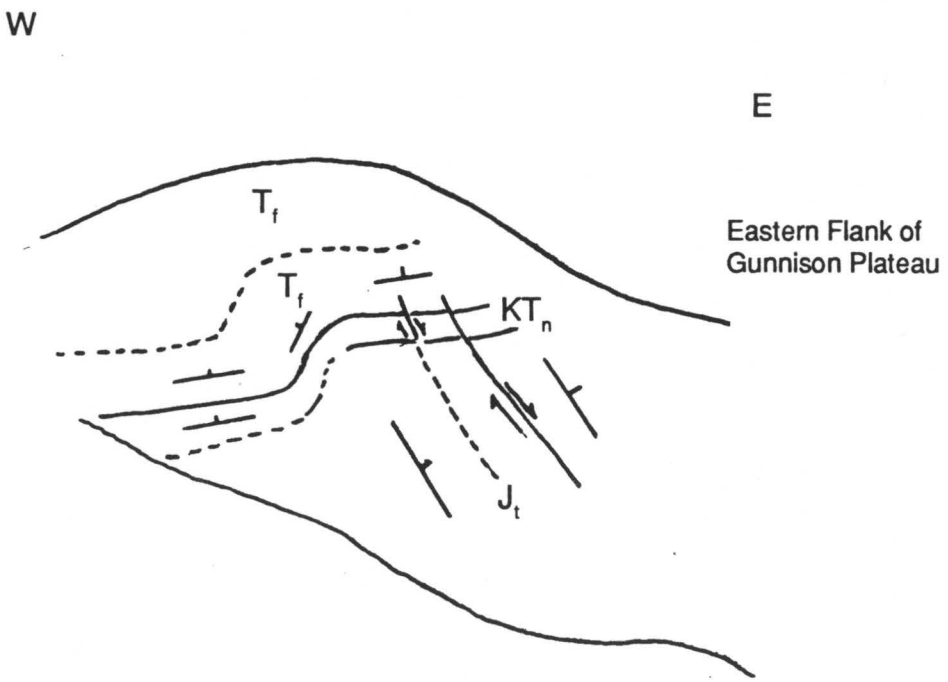

Figure 2b. Tracing of the figure in 2a defining the bedding contacts and the shape of the "S"-Fold.

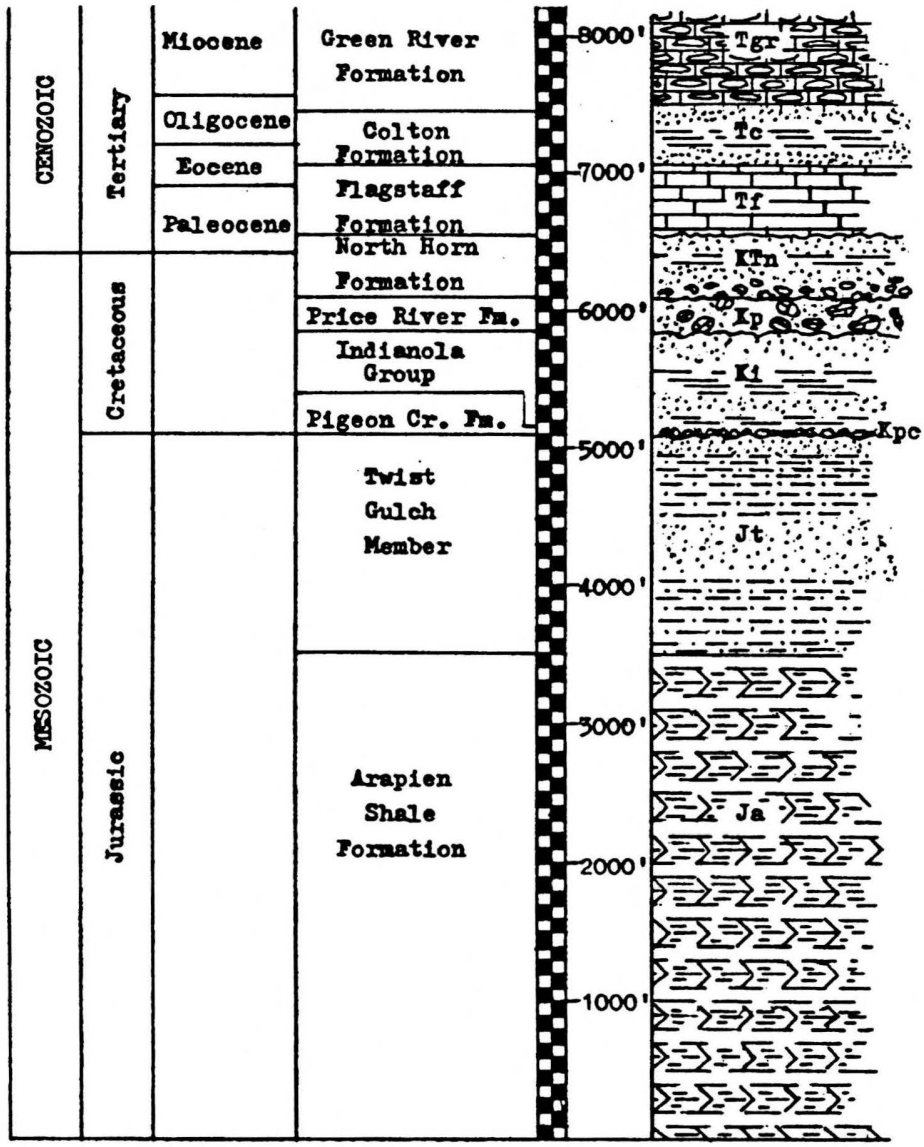

Figure 3. Stratigraphic column of the units of Central Utah. The thickness of the units involved in the "S"-Fold are from Rock Canyon. The other unit thicknesses are from the Rock Canyon area or nearby regions.

The Flagstaff Formation

The Flagstaff Formation was the focus of this study. All field observations and measurements, as well as all samples, were taken from this unit. The Flagstaff is a massive lacustrine limestone that grades upward from a fossiliferous micrite to a sparse biomicrite. Its sand content is moderately high at its base where it is in contact with the North Horn Formation, and decreases upward. The Flagstaff is a resistant limestone as defined by Wanless in his 1979 paper. This means that the unit suffers strain at slightly less resistant internal surfaces and at boundaries with other units. The bulk of the rock remains unchanged. The dominant allochem varies both laterally and vertically in the rock. It contains mostly oncolites and intraclasts, with a small percentage of bivalves and gastropods. The presence of oncolites and intraclasts was significant because of their use for strain analysis. There is also a small percentage of secondary porosity cement present.

EXISTING MODELS OF FOLD DEVELOPMENT

Dr. Edmund Spieker was one of the first to initiate a study of the geology in this region of Utah. His papers on Central Utah covered aspects of the stratigraphy as well as the structure. Three more recent papers written by Witkind(1982), Weiss(1982), and Villien and Kligfield(1986) deal more directly with the structural evolution of the region that involves the "S"-fold in Rock Canyon.

Witkind

Witkind believes that the structure present in Central Utah, including Rock Canyon, was formed by three or four major pulses of salt diapirism (Witkind, 1982). The first of these pulses occurred in the Late Cretaceous and the last one occurred at the end of the Pliocene or the beginning of the Pleistocene. Witkind's model suggests that the folds found in the Sanpete Valley region are upwarpings caused by the mud beds of the Twelvemile Canyon Member (Twist Gulch at Rock Canyon) being forced up by diapiric intrusions of evaporite beds below. These evaporites are part of the Arapien Shale Formation. In this model the beds are gradually warped upward, and then the salt is removed by some action such as dissolution. This causes the mud beds to collapse into the void from lack of support and high angle faults to form in the more competent units above.

Figure 4a shows a set of drawings as Witkind interpreted the structural form. His explanation of folds such as the "S"-fold is that they are formed in stages. Sudden spasmodic upsurges force up mudstones in the Late Cretaceous, folding back overlying strata. The salt is then removed, and the axial part of the fold collapses along high-angle normal

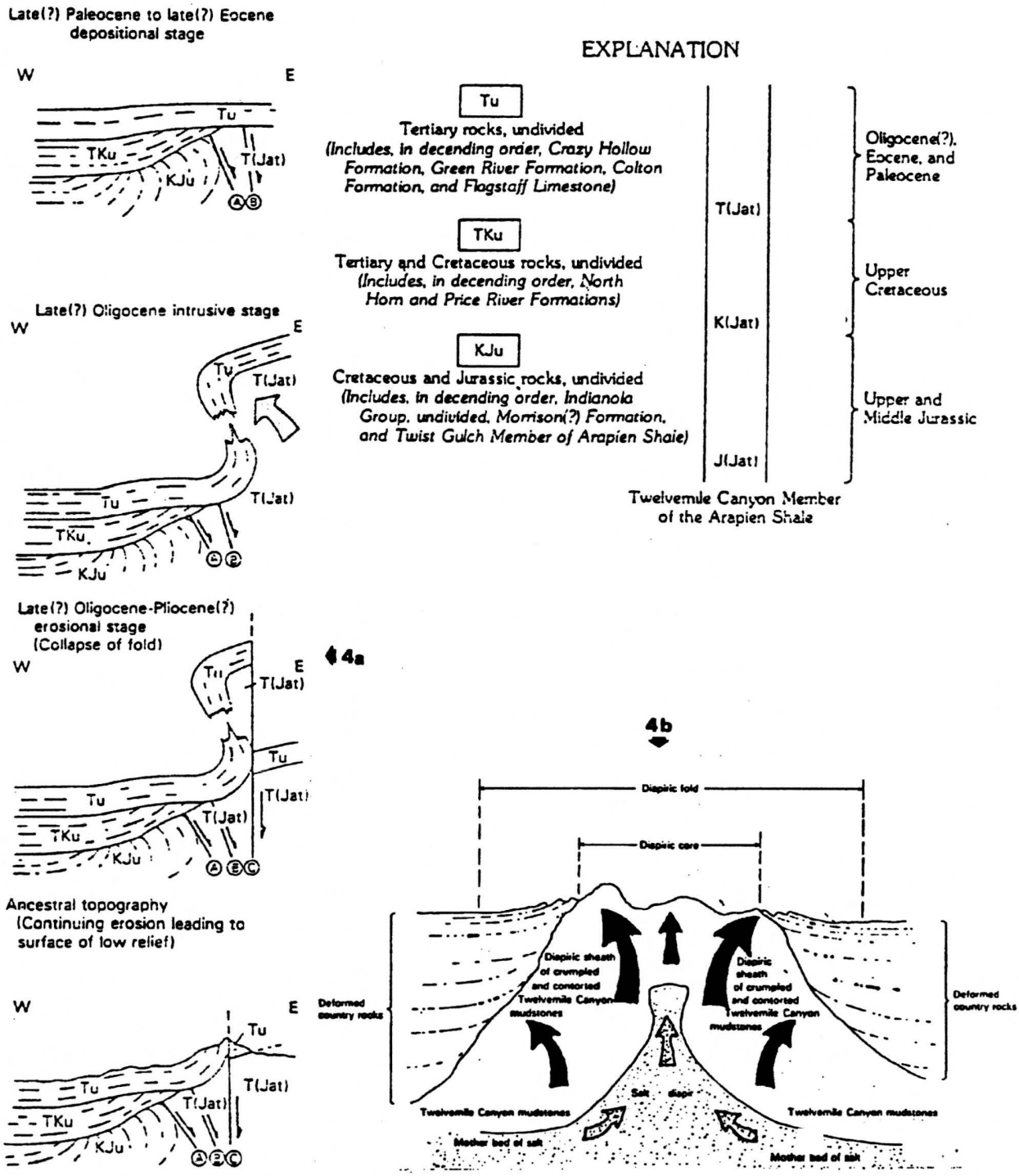

Figure 4a and 4b. 4a is Witkind's model for the formation of folds loke the "S"-Fold by salt diapirs. Figure 4b is Witkind's model for the salt diapirs. Notice the oblique movement of the salts and the sheath rock.

faults. Then the area is eroded flat, leaving different dipping beds across the fault. These stages are repeated three times up to the Miocene, forming a series of unconformities from unit to unit like those seen at Wales Gap north of Rock Canyon. Figure 4b shows a model of Witkind's salt diapirs and their relation to the mudstones and the country rock above. The diapiric sheath pushes the country rock up and back, forming the folds. Strata are subjected to a combined lateral and vertical 'push' from the intrusive salt. Witkind also points out that oil test wells have shown that large amounts of evaporites are present. He calls the source the 'mother lode', which represents the source of the salt for his repeated pulses of diapirism that formed the fold relations such as those at Rock Canyon.

Witkind bases most of the support for his model on the fact that units such as the North Horn Formation (Cretaceous-Tertiary) and the Flagstaff Formation (Paleocene-Eocene)thin laterally, suggesting that they were deposited during formation of these upwarpings. According to Witkind's model, the frontal fold of the Gunnison Plateau formed due to diapiric upwelling of the Sanpete Valley Antiform. Witkind states that, "a salt diapir welled upward either during the Late(?)Oligocene or Early Miocene and forced the mudstones of the Twelvemile Canyon Member to bow up the overlying sedimentary strata and form a fan-shaped diapiric fold"(Witkind, 1982). Steeply dipping beds such as those along the margin of the Gunnison Plateau are interpretted as remnants of the flanks of these diapiric folds. The fault that dropped the Twist Gulch Member adjacent to the Flagstaff was a result of collapse from removal of salt.

Weiss

In his 1982 paper Weiss deals directly with the structure of the eastern front of the Gunnison Plateau. He believes that the Gunnison is close to the locus of the Sevier Arch. The Gunnison contains two synclines with parallel axes. The younger of the two has its axis close to the east side of the plateau and is present at Rock Canyon. This syncline includes the Indianola Group (Middle Cretaceous) and younger units, and has little closure, with the closure decreasing in post-North Horn beds. Weiss also believes that the Gunnison Fault (normal fault) that fronts the plateau is parallel to the Jurassic beds, and that the fault disappears to the south as the throw becomes zero.

Weiss relates the restriction of the "S"-fold to the area between Dry Canyon (half a kilometer south of Rock Canyon) and Rock Canyon to facies changes within the North Horn Formation. The North Horn is normally 40m thick(Weiss, 1982), with a basal conglomerate and rigid bedding. In Dry Canyon the North Horn is a very sandy limestone, and just north of Rock Canyon it returns to the normal interbedded sandstones and mudstones. In Dry Canyon it is less than ten meters thick. Weiss states that the North Horn is weak and flexible in the area between Rock and Dry Canyons, in contrast to the

stiffer well-cemented conglomeratic sandstones that characterize the unit to the north and south. This could have allowed the formation of the "S"-fold to occur more easily and be better developed at Rock Canyon. Weiss attributes the thinning of the North Horn and the formation of the "S"-fold to the Sanpete Valley Antiform (Refer to Figure 1.). As the antiform rose it forced the Jurassic beds against the base of the North Horn Formation, folding the thinner and weaker North Horn westward. The antiform could have formed anywhere from the Late Cretaceous to the Early Paleocene. Weiss attributes some of the abnormal thinness of the North Horn in Dry Canyon to a graben block located at this point, which might have been rotated by the movement of the Sanpete Valley Antiform. Spieker (1949) believed the thinning was due to the horst block which later down-dropped a section that was closer to the antiform axis into place as it is seen today.

Villien and Kligfield

Villien and Kligfield(1986) present a model for the evolution of the Sevier Thrust Belt in Central Utah. They describe this thrust system in terms of the classic pattern of foreland-migrating deformation and deposition, with localized backthrusting in the Sanpete Valley(See Figure 30 later in this paper). The Gunnison Plateau is underlain by duplex structures belonging to the Wasatch Thrust System. There is also a major ramp in the Gunnison Thrust which climbs up section from the Cambrian Shale on the west side of the plateau into the Arapien Shale. Towards the east a series of imbricate blind splay faults branch upwards from the ramp. Continued shortening in the Early Paleocene was compensated for by west-vergent, east-dipping backthrusts of the Wasatch System from the western edge of the Wasatch Plateau across the Sanpete Valley and up the eastern face of the Gunnison Plateau. Villien and Kligfield link backthrusting geometrically to the Wasatch Duplex formation beneath the Gunnison Plateau. Backthrusting is difficult to date because of changing unconformable relations in the area. Along the Gunnison, the Flagstaff and North Horn Formations are conformable at different localities , while on the western edge of the Wasatch Plateau the North Horn-Indianola Unconformity is truncated by the Flagstaff Unconformity. Yet backthrusting is thought to be the cause of the thrusts of Indianola over North Horn in the Sanpete Valley to the south of Ephraim. Villien and Kligfield believe backthrusting could have occurred anywhere from the Late Cretaceous to the Late Paleocene.

Although not explicitly discussed, it is presumable the "S"-fold is a feature that is a result of the backthrusting in Villien and Kligfield's model. It marks where the back-thrust units slid upwards along the face of the Gunnison Plateau. It was buckled by the regional compression. The movement of the backthrust initiated the buckling.

Extension followed backthrusting in the form of listric normal faults beginning in the Late Tertiary. Villien and Kligfield believe these faults may follow Late Precambrian

rifting weaknesses. They also believe that propagation of imbricate splays on the eastern edge of the Arapien Shale caused decoupling of stratigraphy (adjacent to the Middle and Upper Jurassic), allowing the backthrusts to reverse, causing a partial collapse of the region that includes the "S"-fold. This collapse has removed part of the fold from the study site area.

Villien and Kligfield recognize the Sanpete Valley Antiform and believe that the antiform caused the North Horn-Flagstaff Unconformity.. They also say that salt diapirism caused further deformation along planes created by the thrust tectonics. However, they do not believe either was a major factor in the creation of the geologic structure of the region.

MESOSCOPIC OBSERVATIONS

The general shape of the fold is an "S" when viewed looking north, though at Wales Gap Spieker (1949) observed it looking south and referred to it as a "Z"-fold. The fold itself is about 50m high at Rock Canyon. Attitudes were measured along bed B2 between the lower and upper fold closures and plotted on an equal area projection in Figure 5. It can be seen from this that the units of the fold at Rock Canyon do not become overturned, nor do dip directions change from one side of what is being called a hinge to the other at either the crest or the trough. Thus the fold is a west facing monoclinal flexure.

The study of the formation of this "S"-fold centers around the occurrence of stylolites and calcite veins found in the Flagstaff Formation in the fold in Rock Canyon. In the field these stylolites and veins were measured for attitude and frequency. Samples containing intersections of stylolites and veins or just one of the two features were collected from measurement areas. The stations used in the field for measurements were selected based on their position in the fold. Figure 6 shows the field stations and the members mapped within the fold. The folded Flagstaff Formation was divided into four informal members, with mapped contacts at the tops of the marker beds labeled B1 through B4. The beds are identified in the cross section in Figure 7. The majority of the work was done at the stations in the lower hinge or in the adjacent limbs. Stations 1 and 4 were in the lower hinge in beds B2 and B4 respectively, while Stations 5 and 6 were in beds B4 and B2 near the crest. Station 2 in bed B2 was very important because it was along the near vertical limb of the fold between the two hinge zones. Station 3 was the farthest from the fold closure and was used to examine the stylolites and calcite veins away from the hinge zones. Stations 1, 4, and 5 near the hinge zones are important because they are where maximum compression and extension are thought to have taken place in the fold.

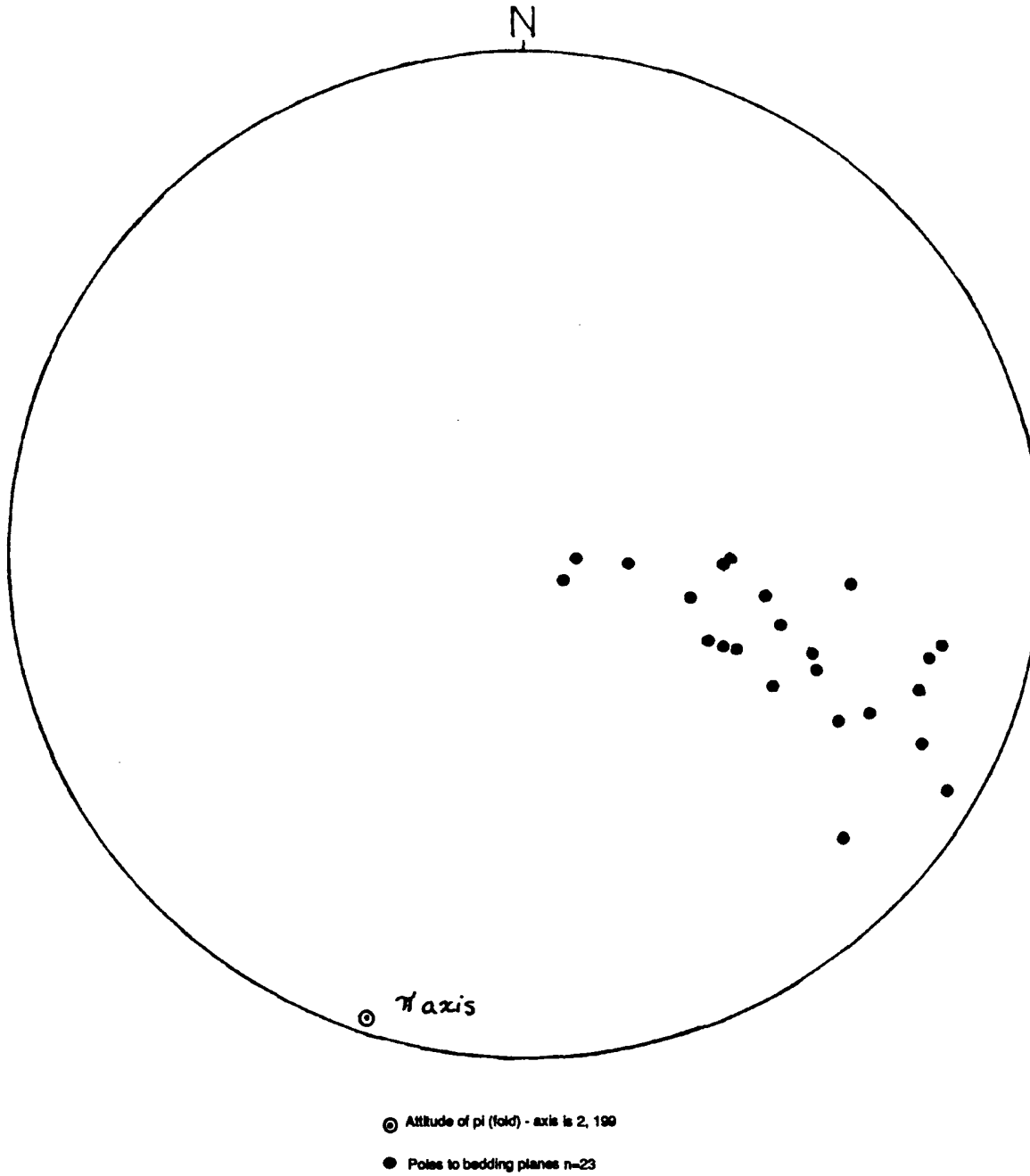

Figure 5. Pi - diagram of bedding attitudes measured from the bottom of the fold to the top. The pi - axis is parallel to the axis of the fold.

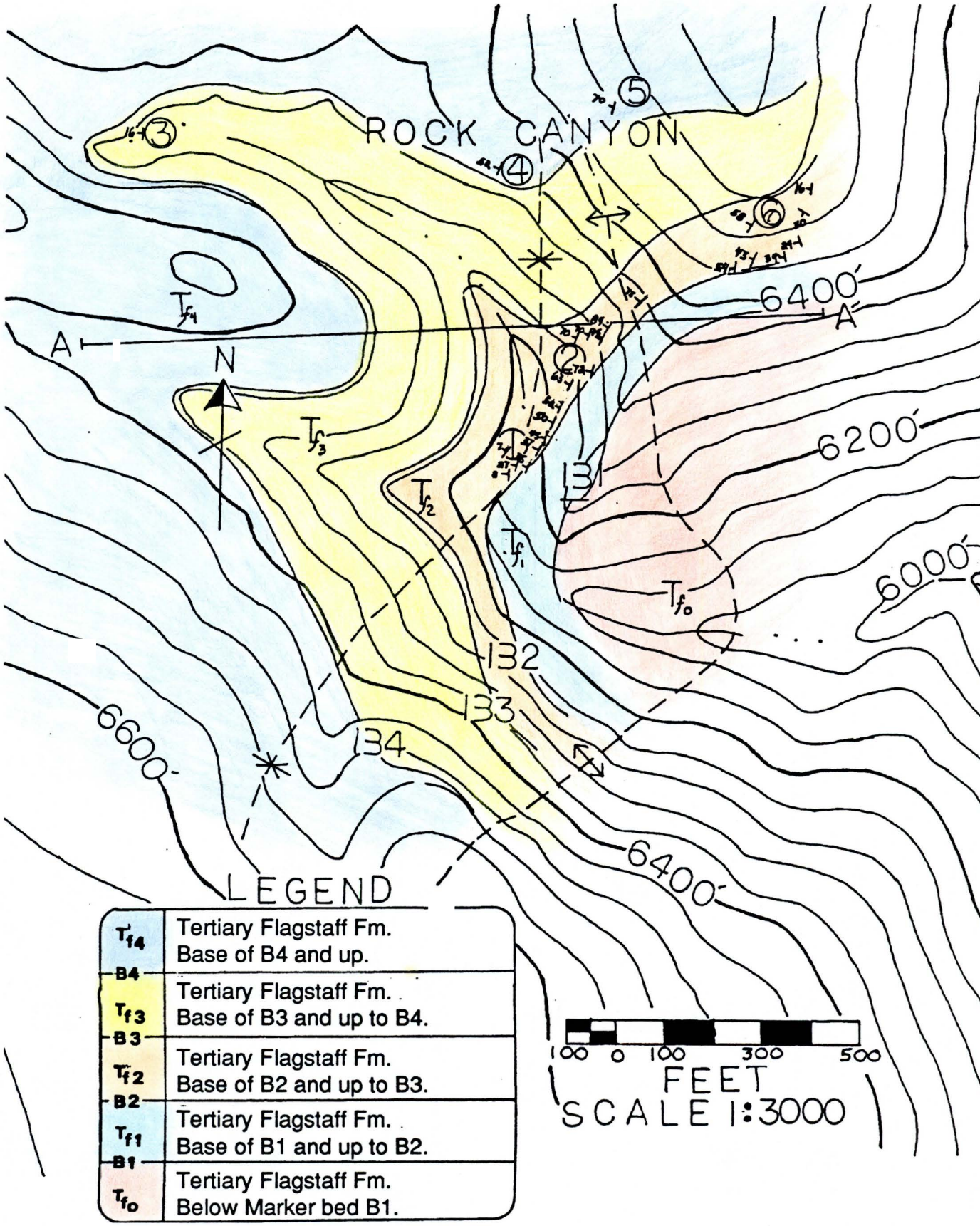

Figure 6. Geologic field map of the study site at Rock Canyon. The stations are marked by the numbers in the circles. Contacts were mapped at the tops of the marker beds.

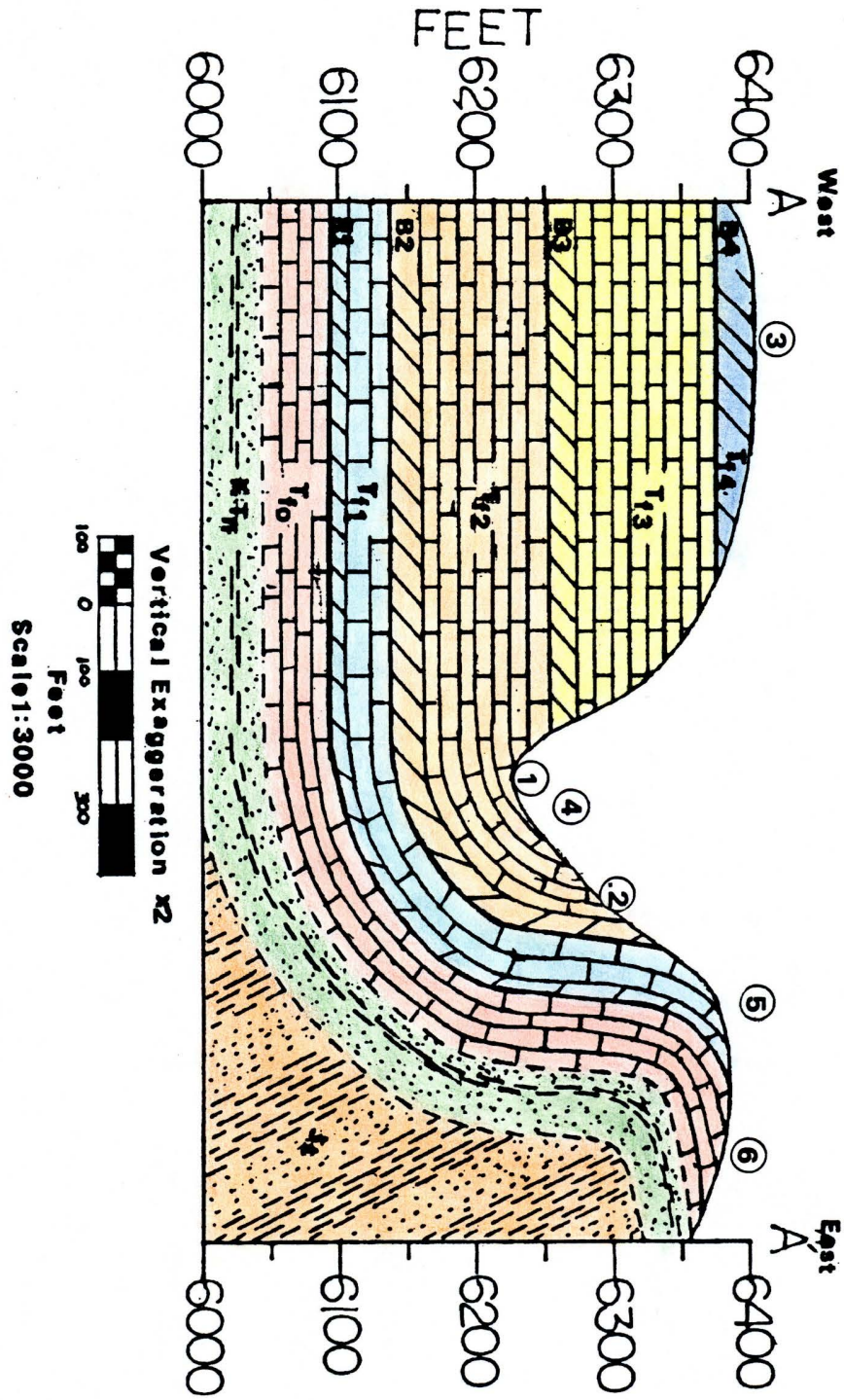

Figure 7. Geologic cross section A-A′ of the study site in Rock Canyon from the map in figure 6.

See following page for legend.

LEGEND

T_{f4} Tertiary Flagstaff Formation, base of marker bed B4 and up.

B4

T_{f3} Tertiary Flagstaff Formation, base of marker bed B3 to B4.

B3

T_{f2} Tertiary Flagstaff Formation, base of marker bed B2 to B3.

B2

T_{f1} Tertiary Flagstaff Formation, base of marker bed B1 to B2.

B1

T_{f0} Tertiary Flagstaff Formation, below marker bed 1.

KT_n Cretaceous - Tertiary North Horn Formation

J_t Jurassic Twist Gulch Member.

Stylolites

Stylolites are pressure solution boundaries where, under compression of the bed, the carbonate was dissolved away leaving a residue of clay and carbonaceous materials. They are post-lithofication features. Merino, et al(1983) state that Dunnington(1967) pointed out that stylolites "... appear to have originated where porosities were originally highest but grain sizes were lowest". Merino, et al (1981) state that in a small volume of rock where the porosity is slightly larger than elsewhere, the local stress borne by the grains is greatest, and thus the local equilibrium concentration of solute in the pore fluid is higher. Diffusion removes solute to areas of lower porosity and equilibrium concentration, which leads to further dissolution and an increase in porosity in the original volume of rock, and leaves the clay and carbonaceous material. Under the action of stress, these porous regions of the rock enlarge to the point that the area physically collapses (Merino, et al, 1983). This feedback mechanism is favored by small grain sizes such as those found in the micritic Flagstaff Limestone.

The stylolites examined exhibited either sinusoidal or irregular waveforms, the majority being irregular. This is common for this type of stylolite that forms perpendicu-

lar to bedding (Nickelson, 1972). The photograph in Figure 8 shows an example of a typical stylolite from the fold. The width of the stylololiltes, the distance across the stylolite from undissolved surface to undissolved surface, varied slightly over short distances at all of the stations. They were fairly continuous over a distance of one-half to three-quarters of a meter along strike.

Spacing or frequency measurements done in the field are presented in Table 1. Frequencies in the field were measured at the stations on the scale of one meter. The average of all the measurements taken at the stations was 5.5/m. Frequencies varied widely at stations within a small area, and no characteristic frequencies were associated with either fold hinges or fold limbs.

Table 1.

Station	Avg. Frequency/m
1	7.26
2	2.00
3	9.80
4	NM
5	3.00
6	NM

NM- Not measured due to erosion of the site.

Table 1. Average frequency of stylolites by stations in the field, measured along one meter traverses.

The attitudes of all the stylolites were plotted on equal area projections for each station, as shown in Figures 9 through 14. The bedding attitude at each station is also plotted. From these plots it can be seen that the stylolites all strike approximately north-northeast, but they dip steeply both to the southeast and the northwest. The parallelism of the stylolites with the "S"-fold axial traces and the eastern flank of the Gunnison Plateau indicates that stylolite formation is linked to that of the fold and related to east-west compression and flattening strain. They are almost perpendicular as a group to the bedding in the limestone. This indicates that the stylolites were a product of layer-parallel compression.

The stylolites were rotated around bedding strike back to their position when the Flagstaff was horizontal. These plots can also be seen in Figures 9 through 14. From these it can be seen that when the Flagstaff Formation at Rock Canyon was horizontal the stylolites all had the same general vertical attitude. This indicates that they were all formed due to layer - parallel compression *prior* to folding. Therefore, lateral compression occurred for a time prior to buckling.

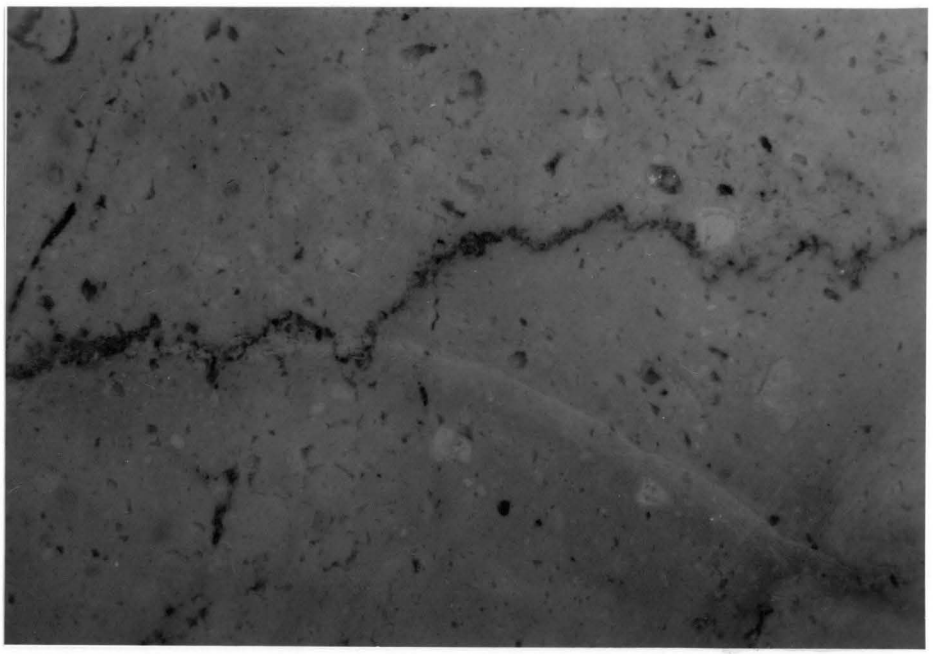

Figure 8. Photograph of a typical stylolite from the study site in Rock Canyon. The sample has been cut to give a planar surface . The long axis of the picture is 14 mm.

Stylolite teeth are interpenetrating columns along the pressure solution surface that form perpendicular to the plane of the stylolite. The photograph in Figure 15 shows these teeth as they appear in the field. These intepenetrating teeth are points of maximum pressure solution and are expected to be parallel to the direction of the maximum compressional stresses(Alvarez, et al, 1976). In most cases teeth were not preserved on the stylolite surfaces, but at Stations 1 and 3 a few were preserved and their attitudes were measured. These were also plotted and rotated about the strike of the bed on equal area plots (Figures 16 and 17). The average orientation from the stylolite teeth points to a maximum compression direction oriented east-west to west-northwest - east-southeast.

Calcite Veins

The morphology of the calcite veins was not variable. They appear in the field as long thin planes of clear calcite. They have smooth to slightly wavy margins with the limestone. The lengths of the veins varies widely from a few centimeters to a few tens of centimeters. The veins occurred in bundles with a spacing of approximately one meter between them. Inside of this zonal arrangement, however, there were no distinctive frequencies.

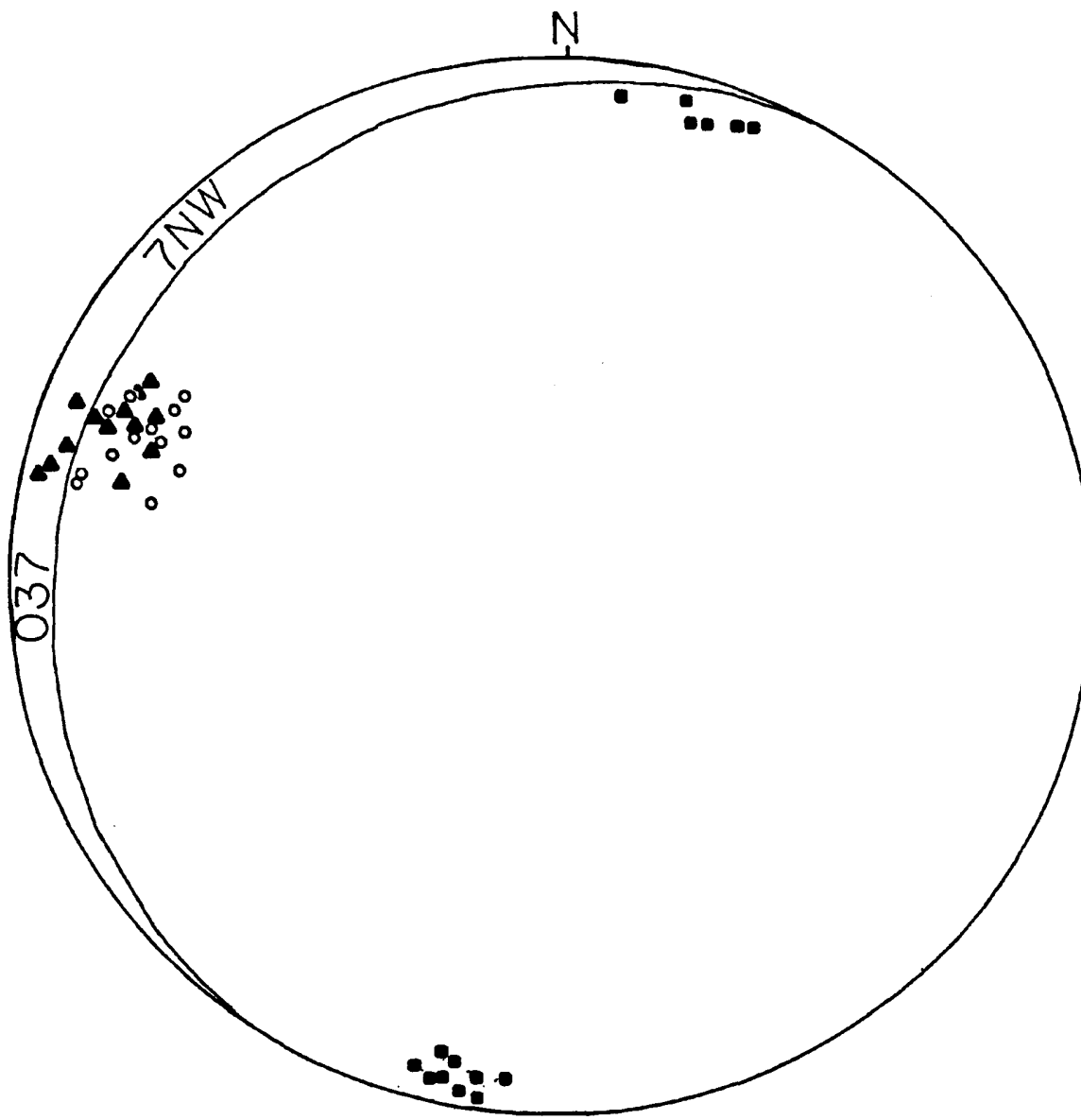

○ Poles of planes of stylolites, n = 13
▲ Poles of planes of rotated stylolites, n = 13
■ Poles of planes of calcite veins, n = 15

Figure 9. Equal area plot of Station 1 (lower hinge in bed B2). Plot shows poles to planes of the stylolites, and the calcite veins, as well as the bedding plane at the station. The rotations are around the line of strike of bedding to restore bedding to horizontal.

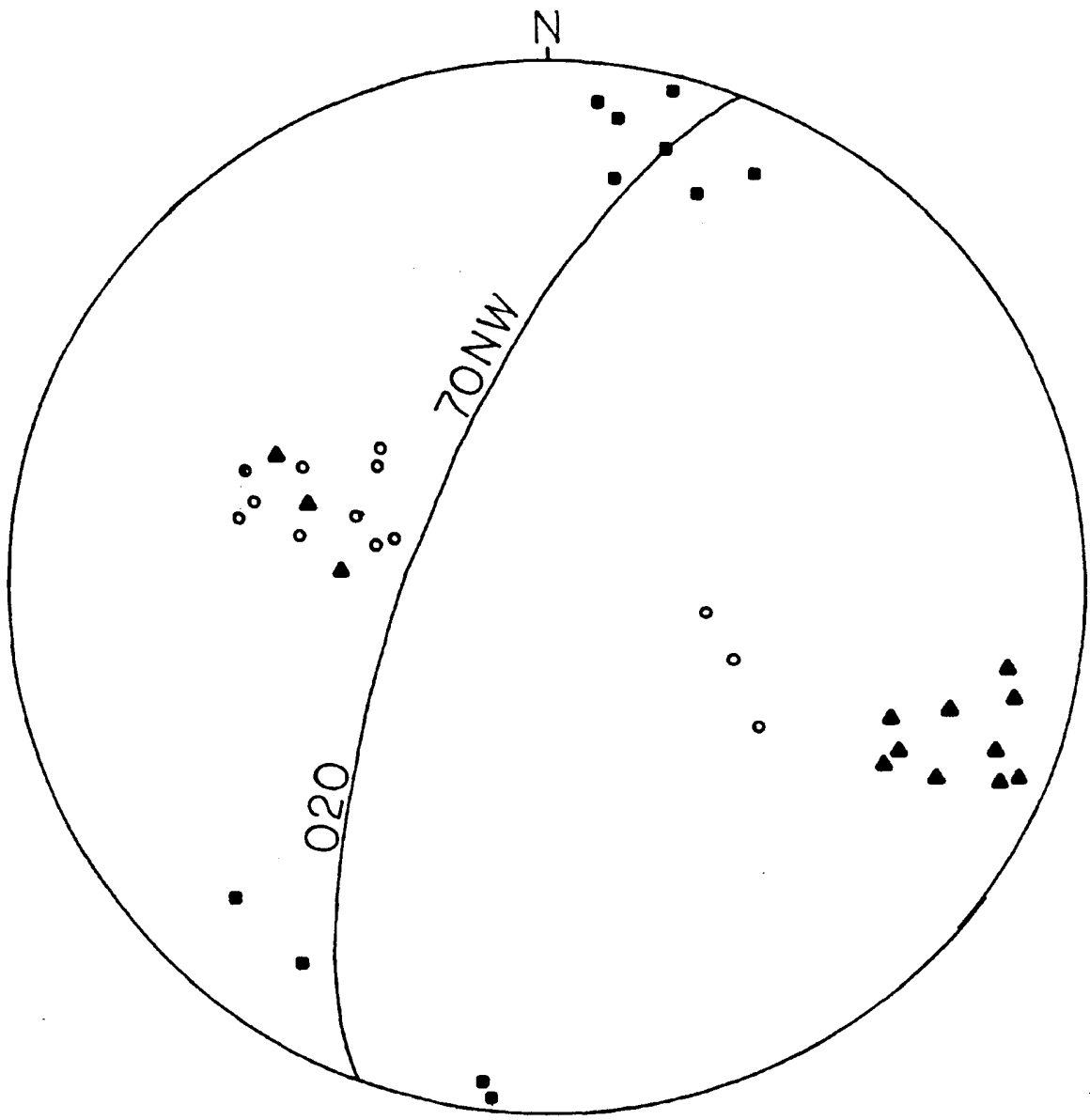

○ Poles of planes of stylolites, n = 13
▲ Poles of planes of rotated stylolites, n = 13
■ Poles of planes of calcite veins, n = 11

Figure 10. Equal area plot of Station 2 (limb between the upper an lower hinges in bed B2). Plot shows poles to planes of the stylolites, and the calcite veins, as well as the bedding plane at the station. The rotations are around the line of strike of bedding to restore bedding to horizontal.

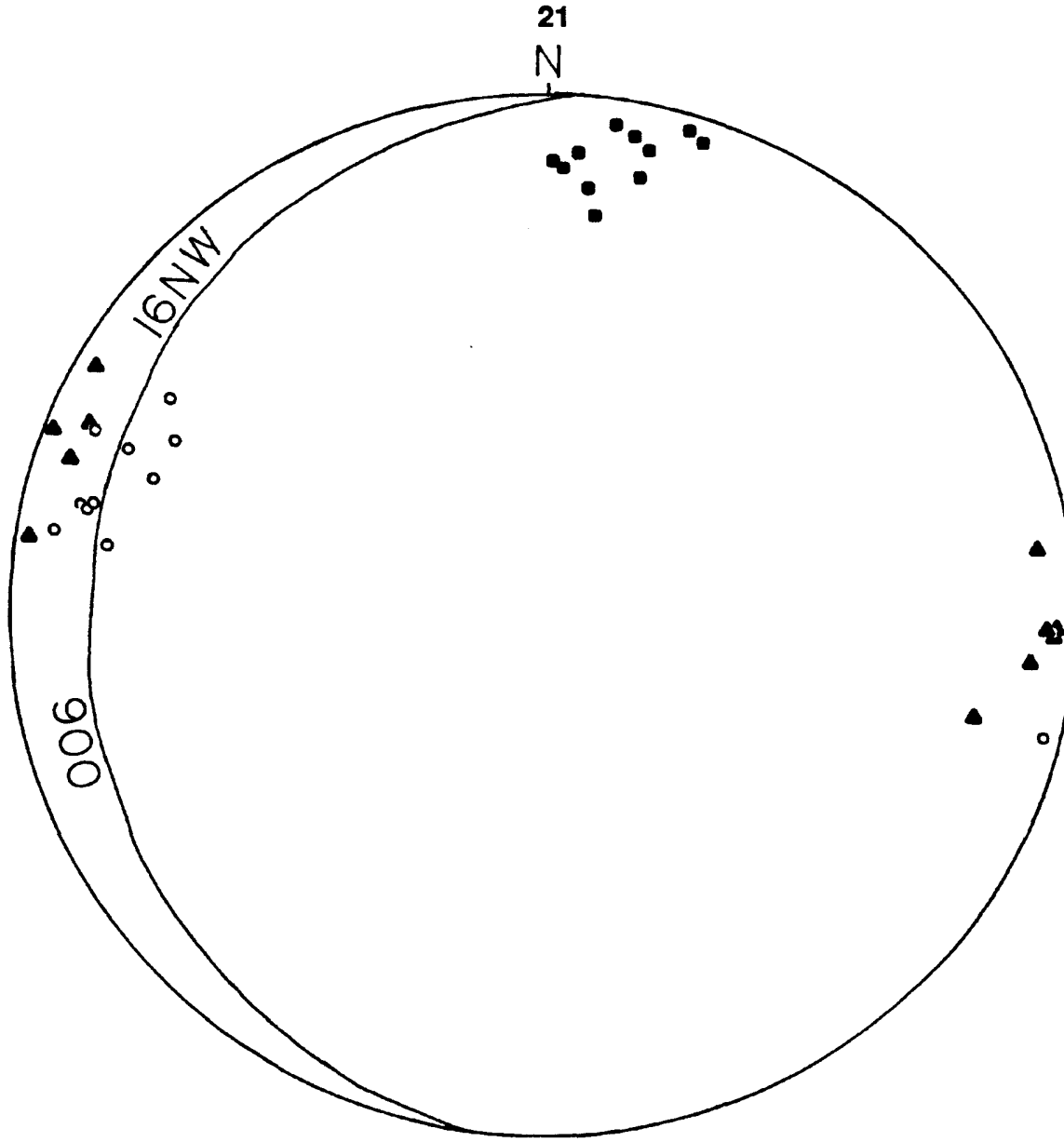

○ Poles of planes of stylolites, n = 11
▲ Poles of planes of rotated stylolites, n = 11
■ Poles of planes of calcite veins, n = 11

Figure 11. Equal area plot of Station 3 (Horizontal limb west of lower hinge in bed B4). Plot shows poles to planes of the stylolites, and the calcite veins, as well as the bedding plane at the station. The rotations are around the line of strike of bedding to restore bedding to horizontal.

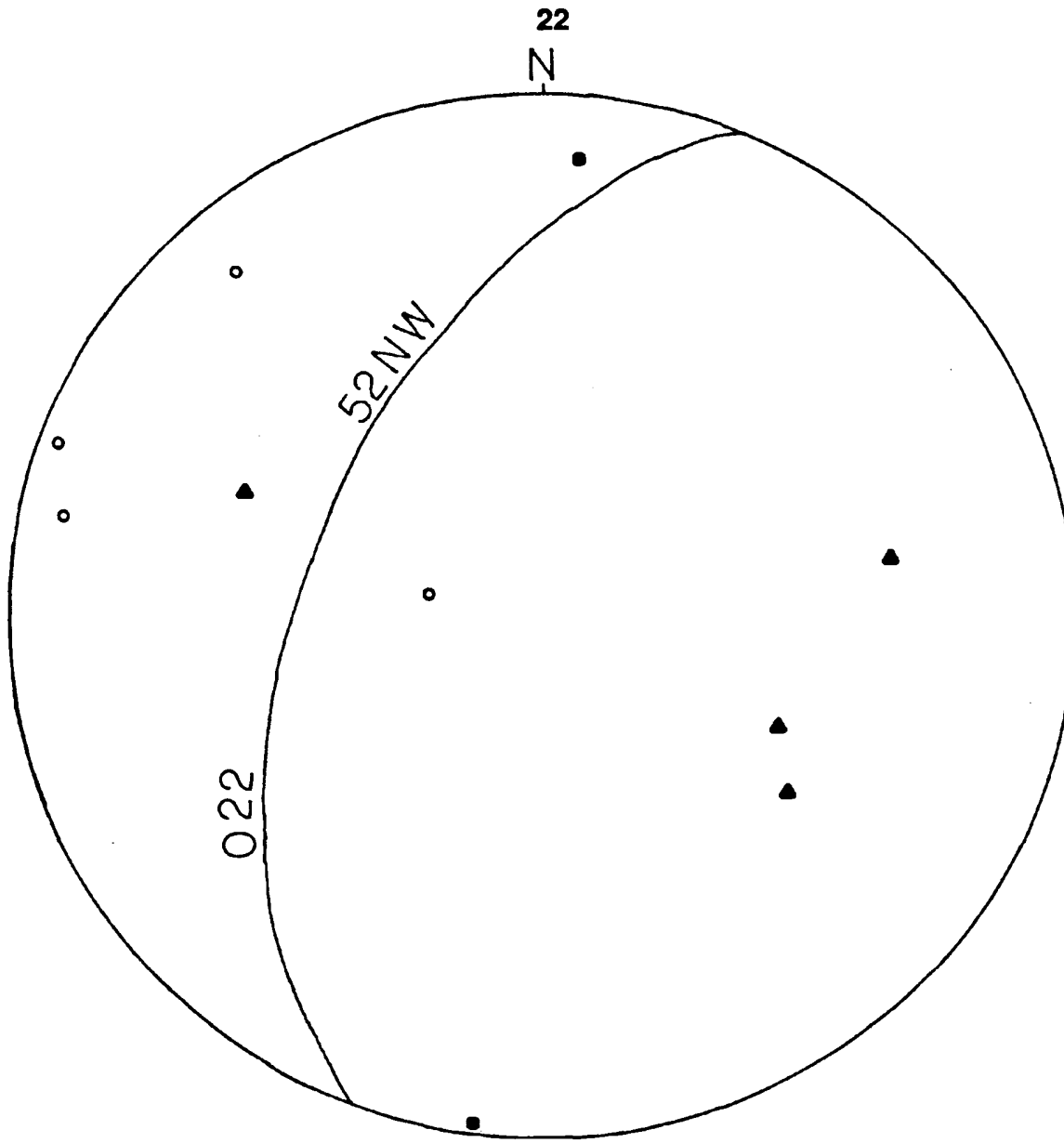

○ Poles of planes of stylolites, n = 4
▲ Poles of planes of rotated stylolites, n = 4
■ Poles of planes of calcite veins, n = 2

Figure 12. Equal area plot of Station 4 (lower hinge in bed B4). Plot shows poles to planes of the stylolites, and the calcite veins, as well as the bedding plane at the station. The rotations are around the line of strike of bedding to restore bedding to horizontal.

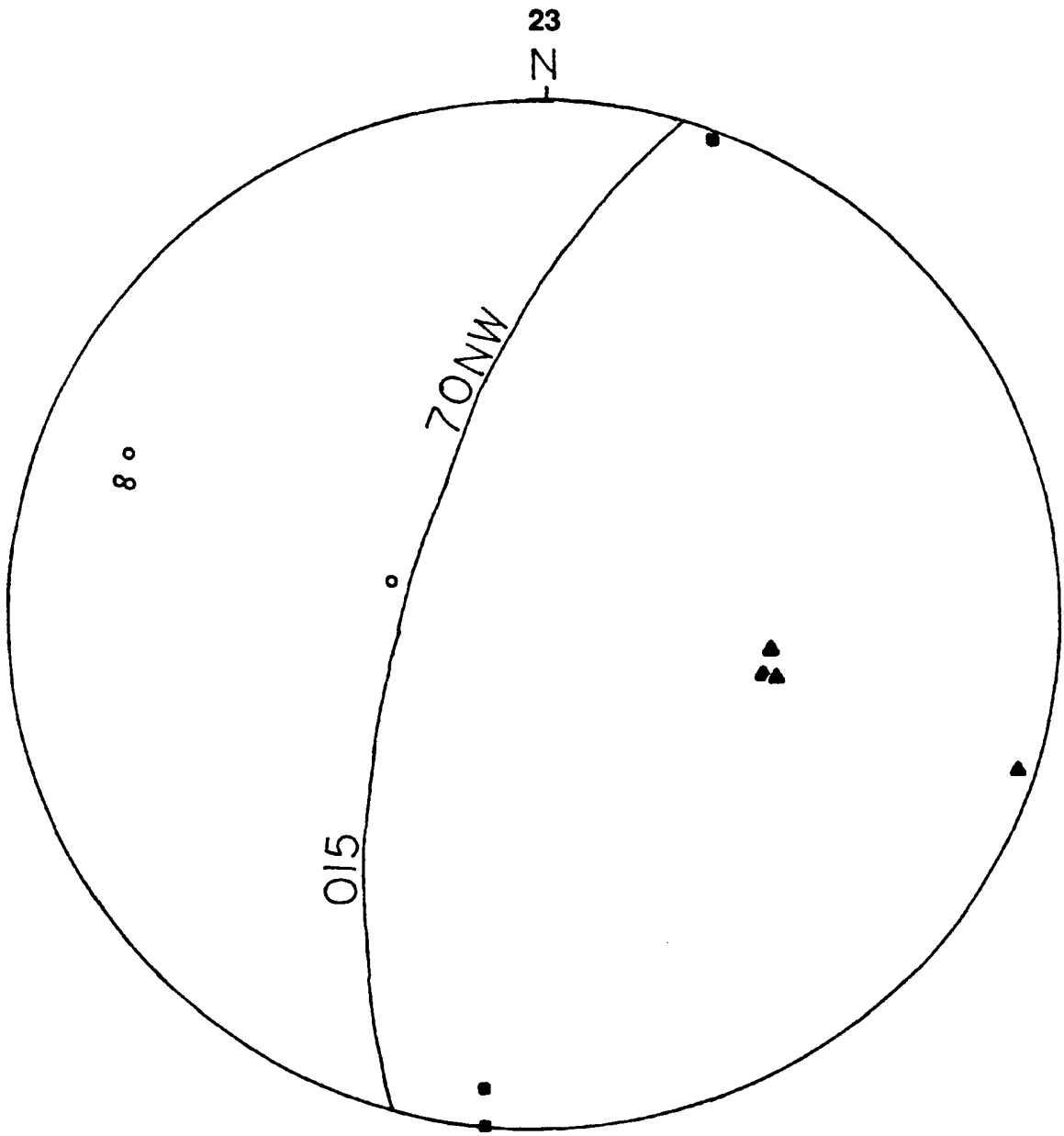

o Poles of planes of stylolites, n = 4
▲ Poles of planes of rotated stylolites, n = 4
■ Poles of planes of calcite veins, n = 3

Figure 13. Equal area plot of Station 5 (east of upper hinge in bed B4). Plot shows poles to planes of the stylolites, and the calcite veins, as well as the bedding plane at the station. The rotations are around the line of strike of bedding to restore bedding to horizontal.

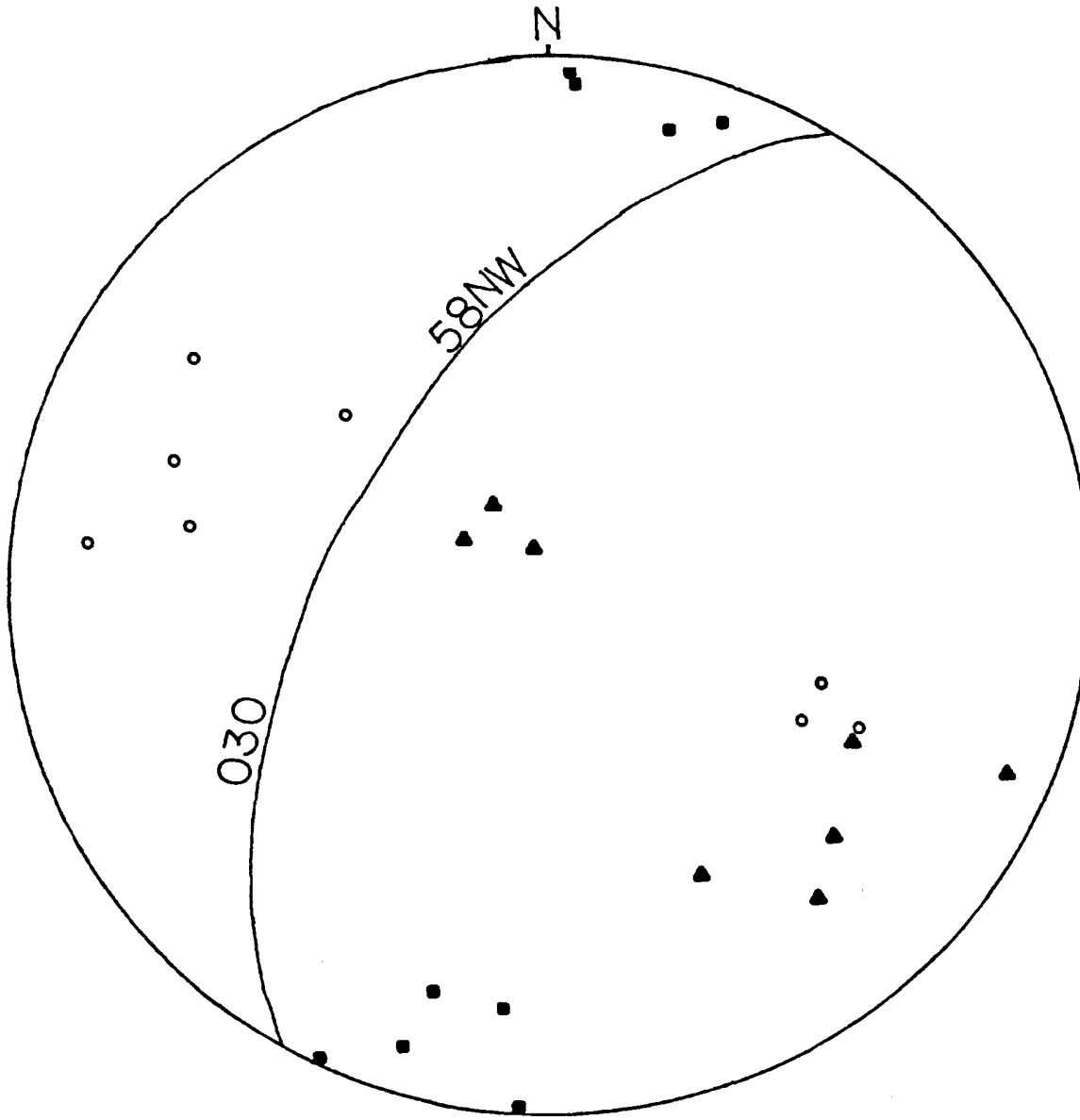

○ Poles of planes of stylolites, n = 8
▲ Poles of planes of rotated stylolites, n = 8
■ Poles of planes of calcite veins, n = 9

Figure 14. Equal area plot of Station 6 (east of upper hinge in bed B2). Plot shows poles to planes of the stylolites, and the calcite veins, as well as the bedding plane at the station. The rotations are around the line of strike of bedding to restore bedding to horizontal.

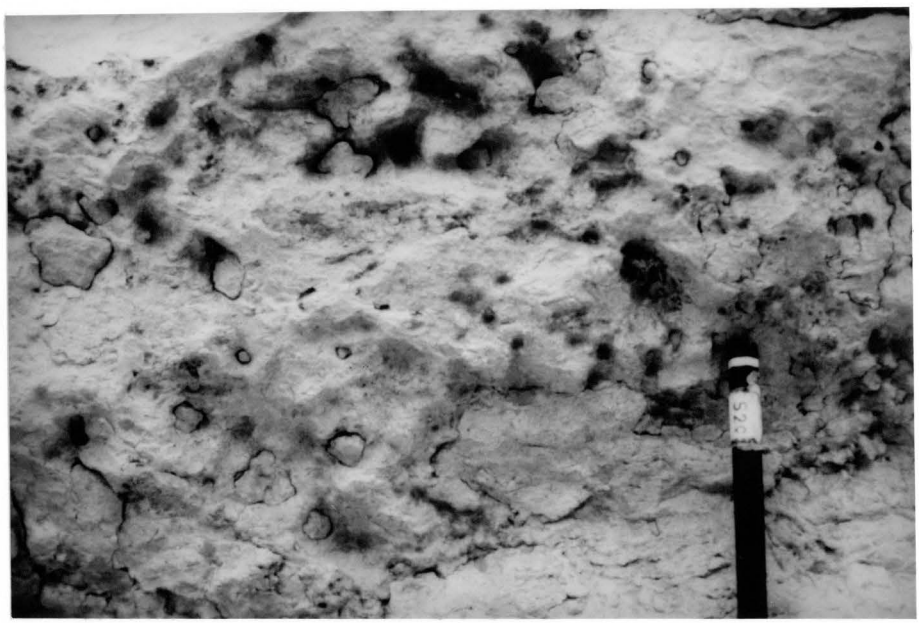

Figure 15. Photograph of the stylolite teeth as they appeared in the field at Rock Canyon.

The attitudes of the calcite veins were measured at each station and plotted in Figures 9 through 14 , showing they all have the same general attitude, regardless of their position on the fold. Their general strike is west-northwest, and they dip steeply to the northeast and southwest, but on average they are near vertical. From the plots it can be seen that the stylolites and the calcite veins are at approximately right angles to each other. This conforms to earlier accepted works as to stylolite and vein orientations in a stress field(Mullenax and Gray, 1984). The veins are thought to be extensional veins. These veins opened up perpendicular to the maximum principle stress direction. Based on the average orientation of the calcite veins the direction of the maximum principle stress was approximately west-northwest to east-southeast, and the least principle sress direction was at 90° to this.

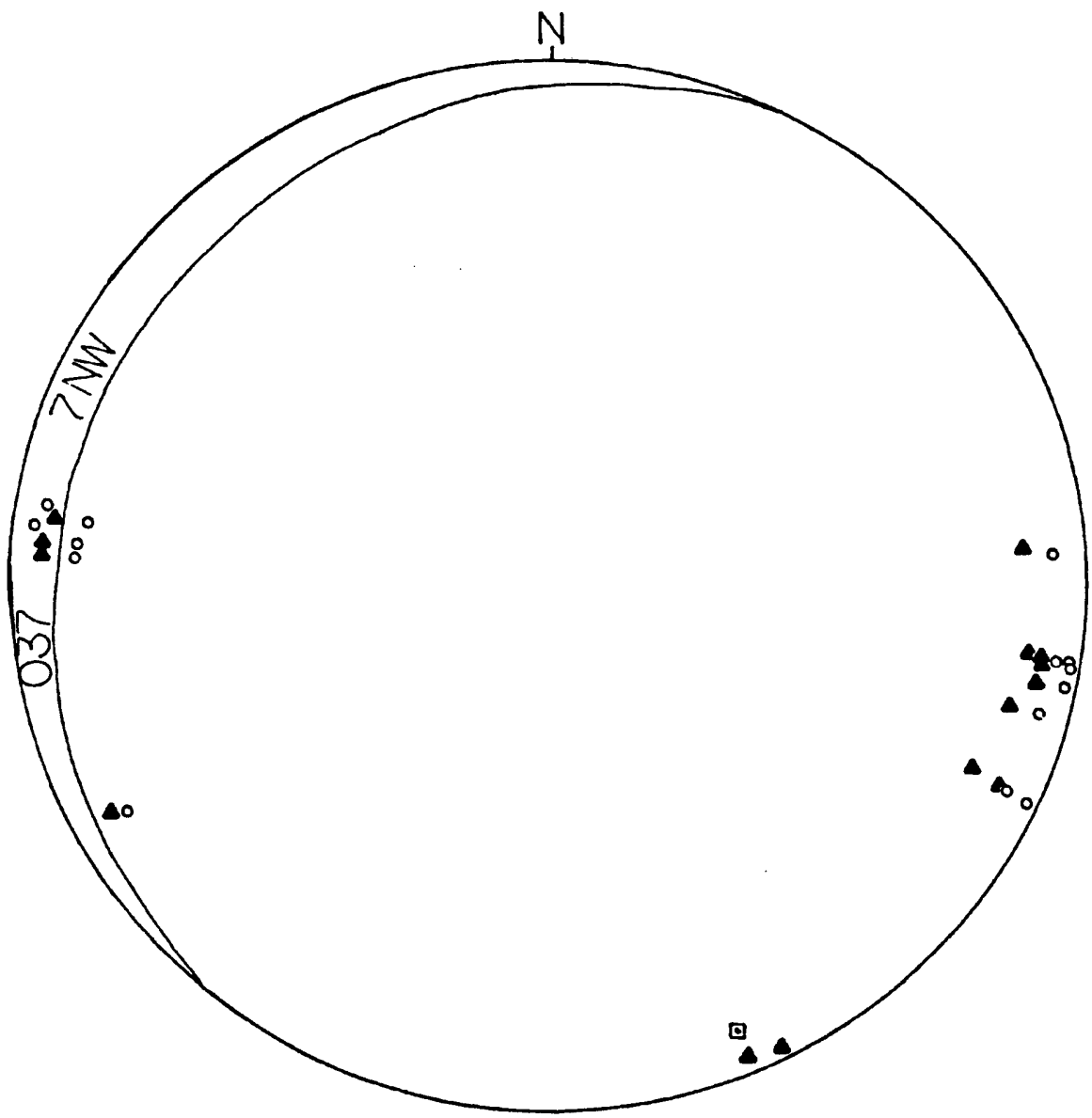

o Trends and plunges of stylolite teeth, n = 14
▲ Trends and plunges of rotations of stylolite teeth, n = 14
⊡ Average orientation of stylolite teeth : 7, 156

Figure 16. Equal area plot of trends and plunges of stylolite teeth and their rotations at Station 1 (lower hinge in bed B2). The rotations are around the line of strike of bedding to restore bedding to horizontal.

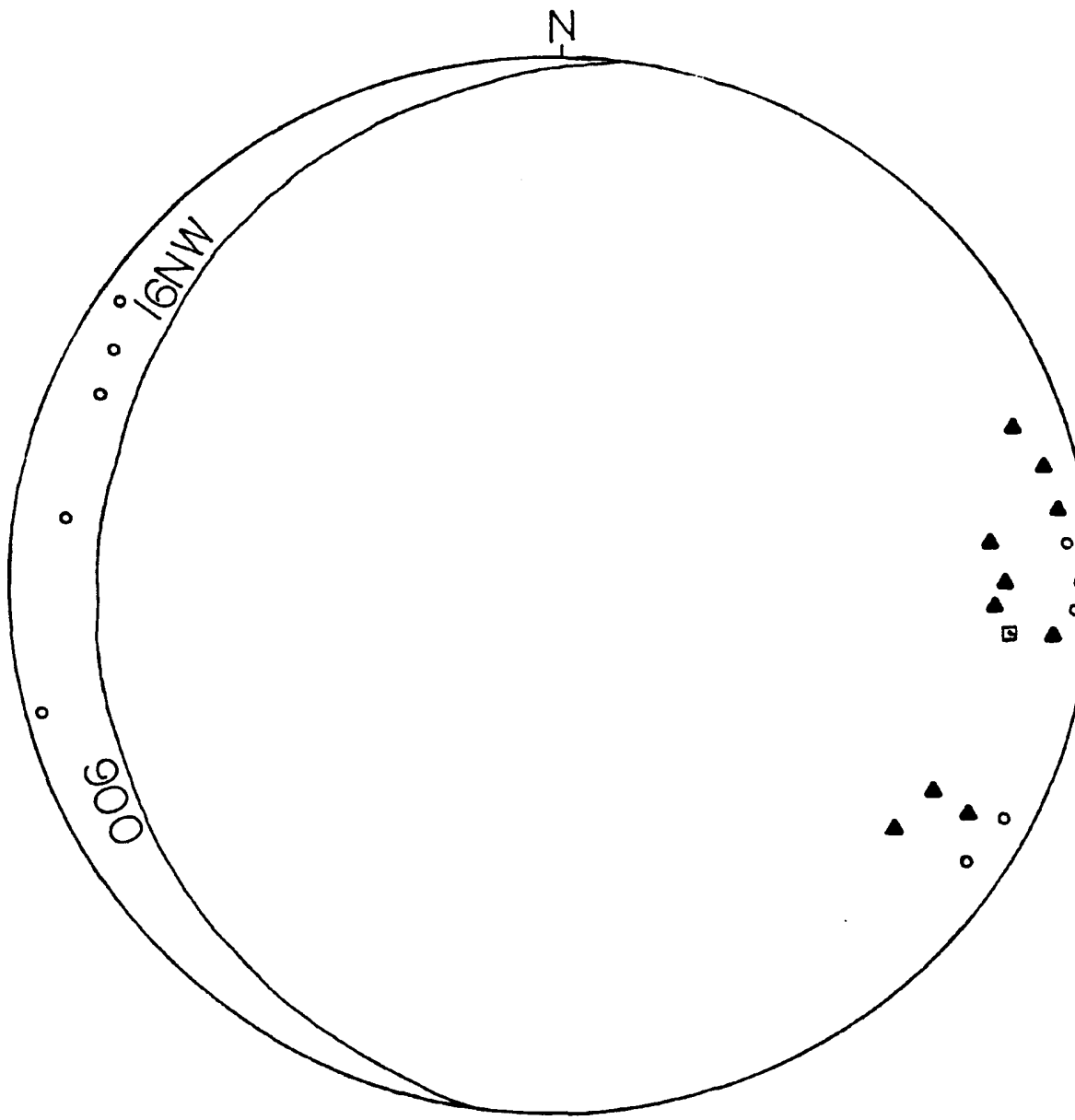

o Trends and plunges of stylolite teeth, n = 10
▲ Trends and plunges of rotations of stylolite teeth, n = 10
⊡ Average orientation of stylolite teeth : 14, 95

Figure 17. Equal area plot of trends and plunges of stylolite teeth and their rotations at Station 3 (horizontal limb west of lower hinge in bed B4). The rotations are around the line of strike of bedding to restore bedding to horizontal.

The measured frequency of the veins is much higher on the average than the stylolites, but like the stylolites the vein frequencies exhibited no consistent relation to any position on the fold and changed rapidly over a small area. They were more consistent than the stylolites. The average was 34.3 veins /m. Table 2. shows the frequencies as measured from different stations.

Table 2.

Station	Avg. Frequency/m
1	31.40
2	NM
3	43.90
4	NM
5	27.50
6	NM

NM- Not measured due to erosion at the site.

Table 2. Average frequency of calcite veins by station measured along one meter traverses perpendicular to strike.

SAMPLING PROCEDURES AND SAMPLE PREPARATION

The samples containing the stylolites and the calcite veins were all cut into slabs and examined under a stereoscope to enhance observation of mesoscopic features. This scale of observation was used to determine if there were any grouping, spacing, or set patterns present that would be lost on the scale of a thin section. This was especially useful on the calcite veins since they are very fine in size and blend in with the limestone.

Oriented samples were collected in the field and labeled to identify their position. A typical label such as B4-5-A shows the three basic components in order: B4 is the marker bed the sample is from, 5 is the station, and the A represents the order in which the sample was taken from the site if there was more than one sample removed.

Thin sections were cut from the slabs after the mesoscopic study. Slabs labeled "A" were cut perpendicular to both the stylolites and calcite veins, slabs labeled "B" were cut perpendicular to the stylolites and parallel to the calcite veins, and slabs labeled "C" were cut perpendicular to the calcite veins and parallel to the stylolites. The sections that contain stylolites have been impregnated to maintain the integrity of the clay material in them. The thin sections are oriented by a two-notch system illustrated in Figure 18. Two

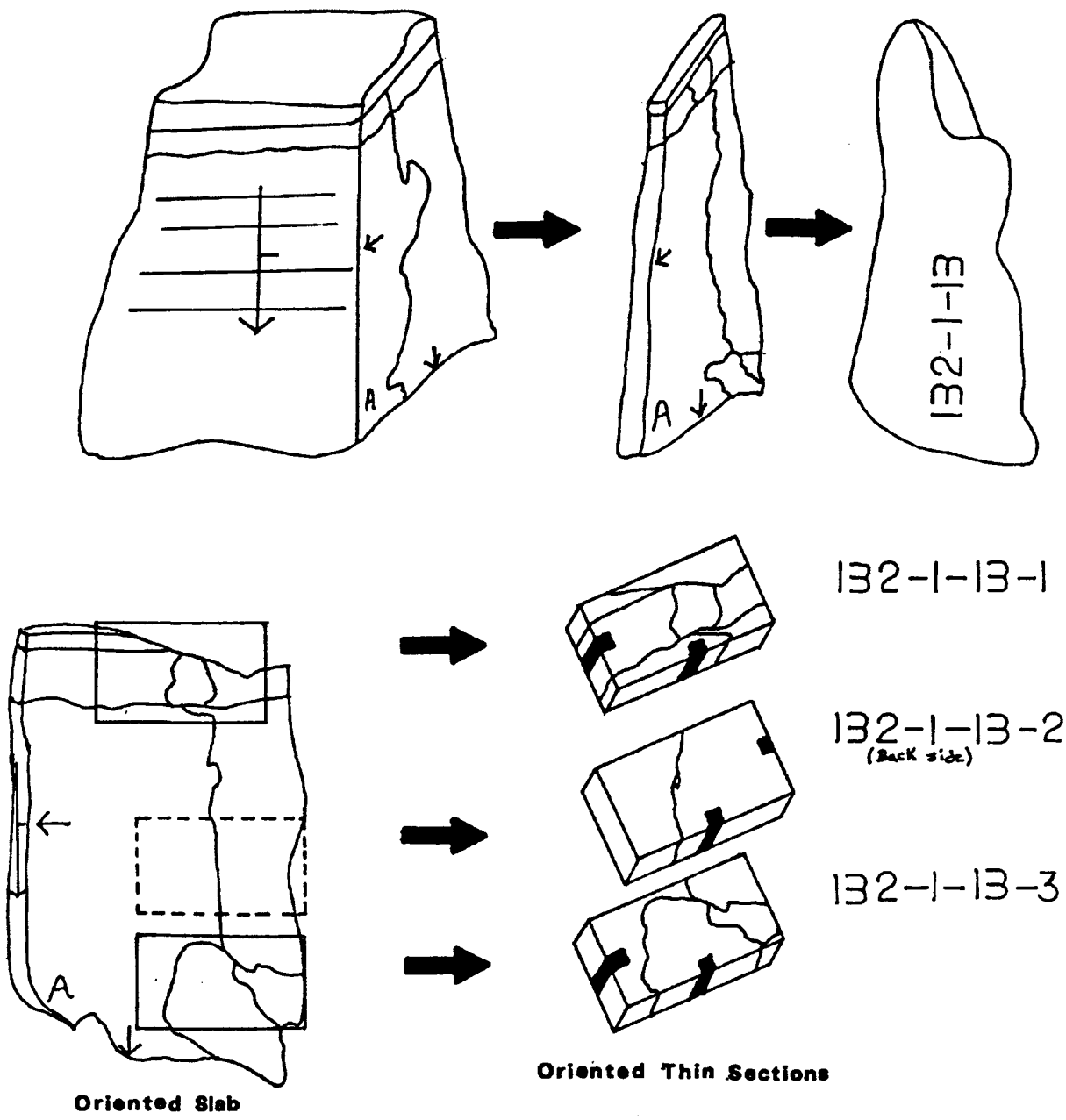

Figure 18. Diagram showing the orientation system used to cut samples into slabs and thin sections.

notches were cut in the thin section chips to indicate their orientation, including one in the direction of the face with the orientation marking and the other pointing along strike or dip, or both pointing along strike and dip, whichever set is appropriate. Table 3. shows a complete listing of stations, showing their positions in the "S"-fold, the samples that were collected there, and the thin sections that were cut from them.

Table 3.

Station	Marker Bed	Location on Fold	Sample	Thin Sections
1	B2	lower hinge	B2-1-A	B2-1-A
		or syncline	B2-1-B	B2-1-B-1
				B2-1-B-2
				B2-1-B-3
			B2-1-C	None
2	B2	limb between	B2-2-A	B2-2-A
		the upper and low-	B2-2-B	None
		er hinge zones	B2-2-C	None
3	B4	horizontal limb	B4-3-A	B4-3-A
		west of lower	B4-3-B	B4-3-B
		hinge	B4-3-C	B4-3-C
			B4-3-D	B4-3-D
4	B4	lower hinge	B4-4-A	B4-4-A
		or syncline	B4-4-B	B4-4-B
5	B4	on limb to east	B4-5-A	B4-5-A-1
		of upper hinge		B4-5-A-2
6	B2	on limb to east	B2-6-A	B2-6-A-1
		of upper hinge		B2-6-A-2

Table 3. This table shows a listing of slabs and their thin sections by stations and their location on the fold.

MICROSCOPIC OBSERVATIONS

Slabs

Both the slabs and the thin sections were examined under the microscope. The stereoscopic examination of the slabs did reveal some features not observed in the field. It showed that in the majority of the stylolite-calcite vein intersections, the stylolite was cut by the vein. There were observed, however, crosscutting relations where the stylolites cut the veins. This indicates that at least for a short period of time the stylolites and the calcite veins formed contemporaneously. Since the majority of the stylolites observed were cut by calcite veins, this gives the stylolites a generally older relative age to the veins. The photograph in Figure 19 shows the character of these stylolite - calcite vein intersections as seen in the field. Figure20 gives a closer view of these intersections under a microscope. Nowhere was it found that a calcite vein was cut by another vein or a stylolite cut by a stylolite. Both the veins and the stylolites exhibited branching. The examinations also showed that the traces of the stylolites and the calcite veins were generally straight, and that they were continuous on the scale of the slabs (10 - 25 cm).

The lower limit of the widths of the stylolites and calcite veins was not measurable on this scale, but the upper limits were determined. On this scale the stylolites were observed to range from <0.5mm to 1mm, with some localized bulges up to 3mm across. The calcite veins ranged from < 0.5mm to over 5mm. This is only a minimum estimation of the upper limit because veins were found of this width that were not completely preserved.

The examination for spacing patterns was more detailed on this scale than in the field. Both the stylolites and calcite veins showed a general spacing set over a traverse of one meter in the field. These 'bundles' were not observable on the scale of the slabs. Where more than one stylolite was found on a slab the spacings ranged from two millimeters to twenty centimeters. The spacings on the order of millimeters may just be branches of the same stylolite, with the junction point cut off when the slabs were cut. Sample B2-1-C showed three stylolites with a spacing of approximately 1.5cm between each, but a fourth stylolite was present at one side at a spacing of only 2.5mm. However, this again may represent a branch. No pattern was observed that held from slab to slab.

The calcite veins did not exhibit a consistent spacing pattern from sample to sample outside of the one meter 'bundles' either. Three samples did show a relationship that may represent a pattern. Samples B2-1-A, B4-3-C, and B4-5-A all showed sets of four calcite veins inside a traverse of 1.75 to 2.00mm, or a spacing of approximately 0.50mm.

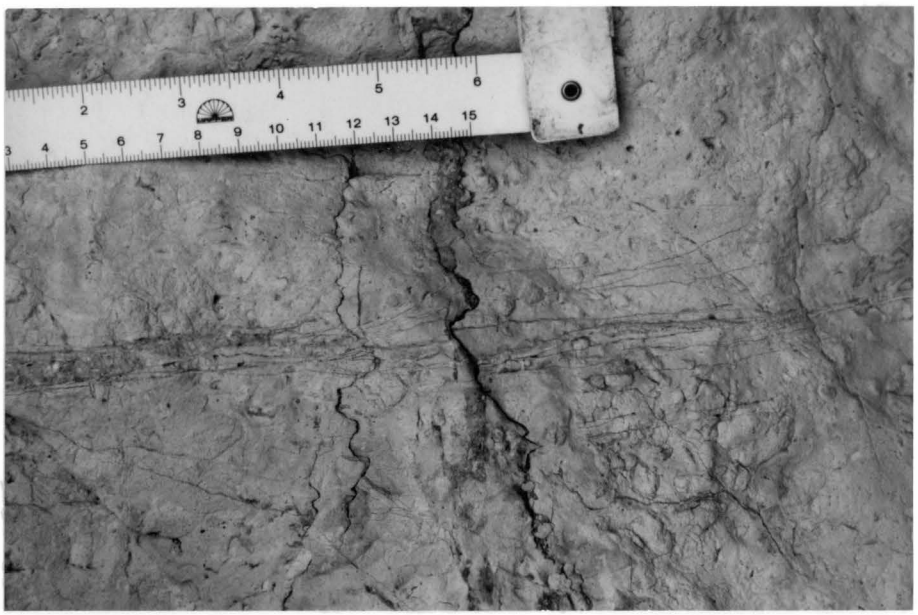

Figure 19. Photograph of the stylolite - calcite vein intersections as they appeared at the study site in Rock Canyon.

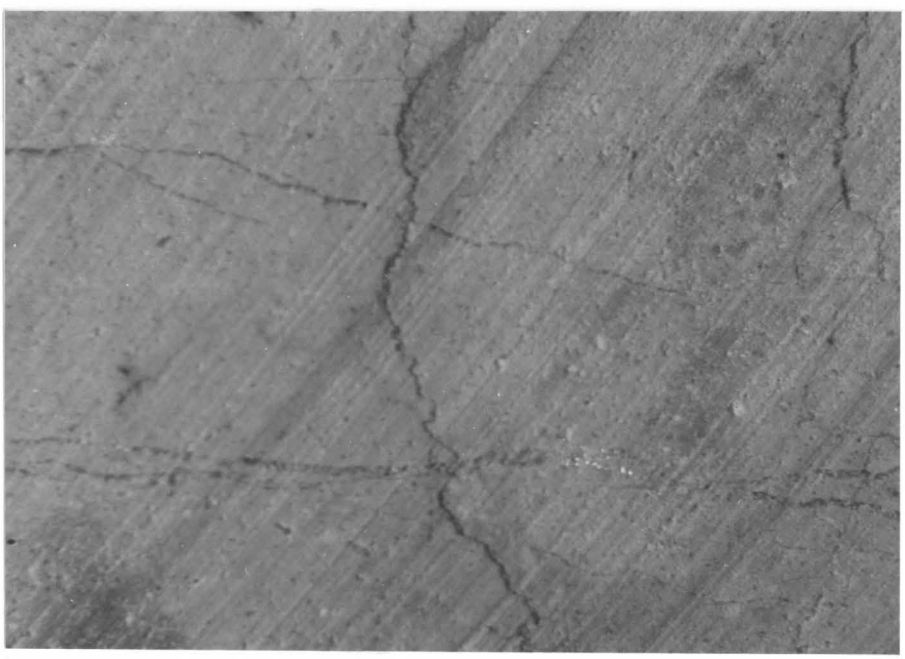

Figure 20. Photograph of the stylolite - calcite vein intersections as they appeared on the slabs under the stereoscope. The long axis of the picture is 18mm.

The stereoscopic examination also revealed the internal structure of the calcite veins. The veins have a wavy planar boundary with the surrounding limestone. The photograph in Figure 21 illustrates this character of the calcite vein-limestone boundaries. At this scale the calcite in the veins appears to be interlocking blocks of sparry calcite, not fibrous as might be expected for extensional veins(Mullenax and Gray, 1984).

One interesting fact that the stereoscope brought out was the relationship of stylolites and calcite veins to 'rip-ups' present in the limestone. 'Rip-ups' are semi-consolidated mud intraclasts that have no consistent shape or size. The calcite veins merely cut through them or followed their boundaries, whereas the stylolites truncated them. Figure 22 shows a picture of a 'rip-up' cut by a vein and truncated by a stylolite. The center of the 'rip-up' has been dissolved. By finding the missing volume of the 'rip-ups' due to pressure solution along the stylolites strain could be estimated, but the 'rip-ups' are unreliable for measurement because their original shapes are indeterminate. The 'rip-ups' were traced and their long axes drawn in, which showed there was no preferred orientation, indicating that there was little or no bulk flattening strain in the limestones, and that shortening was accommodated by the stylolites alone. Oncolites were also found in this unit that were spherical (Kulpanowski and Zawiskie, 1986). Axial ratio measurements confirmed this, again proving there had been no penetrative deformation. If there had been, the oncolites would not have remained spherical.

Thin Sections

The microscopic examination of the thin sections supported much of what was observed before on the mesoscopic scale and added to it. It showed that the limestone was flattened only by pressure solution along the stylolites. The unit did not suffer any measurable amount of penetrative ductile deformation. Shell fragments in the limestone do not show any deformation. This concurs with the early findings based on the rip-ups found in the rock.

Stylolites

The material filling the stylolites is dominately clay, but on the microscopic level it was also observed that many of the stylolites contained fragments of quartz and carbonate(See Figure 23 later in this paper). The quartz was most abundant and was particularly found where the stylolites were widest. This indicates that the quartz was an insoluble component in this system. The quartz grains were originally distributed

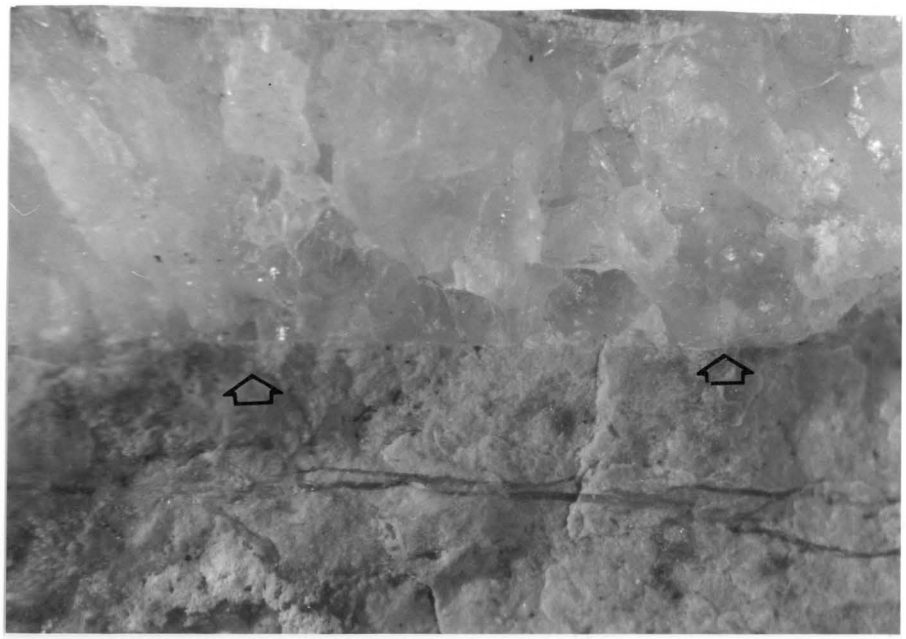

Figure 21. Photograph of the slightly wavy planar margin of the calcite veins. The vein on top is anomalously thick. Long axis of the picture is 14 mm.

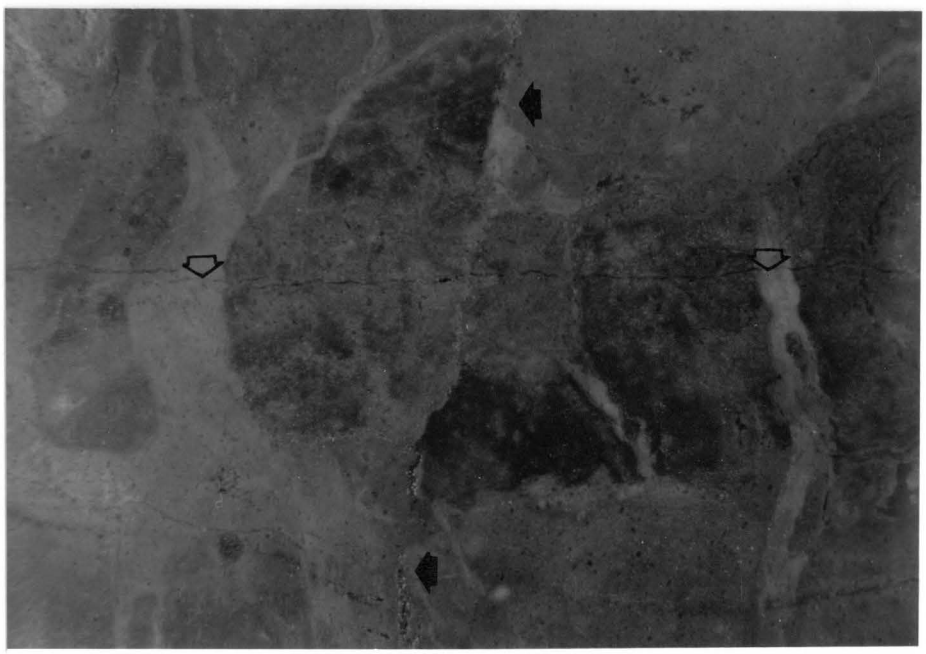

Figure 22. Photograph of a 'rip-up' in the limestone that has been truncated by a stylolite (black arrows) and cut by a calcite vein (outlined arrows). Notice the mismatched boundaries of the 'rip-up' across the stylolite, showing that material has been removed by pressure solution. Long axis of the photo is 14mm.

throughout the limestone matix. Their concentration in the stylolites is evidence that the enclosing carbonate was dissolved and pressure solution occurred there.

The stylolites are more continuous than the calcite veins, and are continuous on the order of the length of the thin section. The stylolites terminate by tapering out to points, becoming thinner towards these terminations. No regular spacing or zonal arrangement was apparent on this scale, as on most of the thin sections only one stylolite was present. If there is a spacing set present, it is on a scale larger than the thin sections and the mesoscopic samples. The regularity(spacing) of stylolites over a traverse can vary by a factor of 2 to 3 between stylolites(Merino, et al, 1983), and studies show spacings can range from 0.002 to 28cm in carbonates (Merino, et al, 1981). This means that even though a regular spacing was not determined on the scale of the slabs or the thin sections, there still could have been one on a larger scale. For the purposes of strain measurements, the stylolites were considered to occur in bundles measuring one meter across.

Even on the microscopic level, the teeth on the stylolites were difficult to observe and measure. On this scale precision of width measurments was much better than on the mesoscopic level. The width of the stylolites varies from less than 0.005mm to 0.5mm, with the localized bulges of three millimeters.

Additional evidence for shortening by pressure solution along the stylolites included the presence of truncated oncolites. On this scale it could be seen that segments of oncolites were missing across stylolites. Their spherical shapes made it easy to see where parts were missing, and truncations only occurred along the trace of the stylolites. No oncolites were found away from a stylolite that were not entirely intact. These missing parts are proof that shortening by pressure solution shortening occurred perpendicular to the plane of the stylolites.

One aspect of the stylolites in the rock that was brought out by the microscope was the presence of a second set of stylolites in three of the thin sections, B2-1-A, B2-1-B-3, and B4-3-C. This second set is made up of the smallest-sized stylolites. This set is at right angles to the trend of the main set observed in the field. Because this second set was so much finer and thinner, less extensive, and branched off the main set, it is believed the set is secondary to the main set. Figure 23 shows a photograph of the two sets of stylolites. The presence of these minor stylolites may indicate that the compressive stresses were reoriented during the later stages of deformation. Another possibilty is that they were caused by heterogeneites within the limestone that reoriented the local stress field.

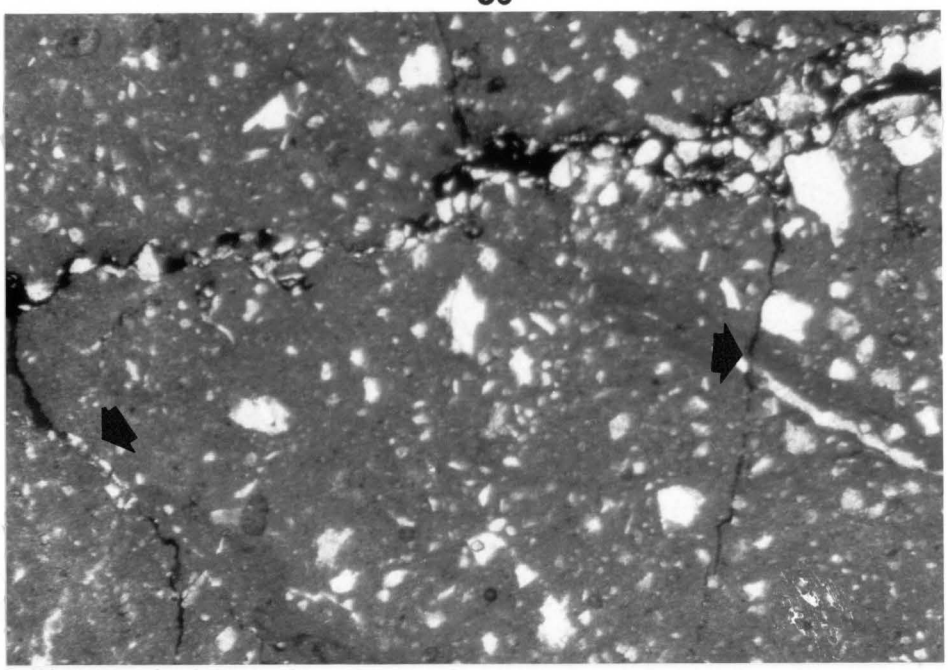

Figure 23. Photograph of the main and secondary sets of stylolites. Notice the concentration of insoluble quartz grains in the main stylolite in the upper right corner. The long axis of the picture is 2.1 mm.

Calcite Veins

The calcite veins were all made up of blocky calcite as had been observed in the larger veins before. However, the long axes of many of the calcite crystals in the veins were perpendicular to the walls of the veins. This indicates that even though they are not fibrous, they still formed by extension. They are an infilling of material in the void of the cracks that opened in the rock due to extensional strain. This blocky calcite agrees with the stylolite-vein work done by Mullenax and Gray(1984). They also found that calcite veins in units that were folded by similar means to the "S"-fold exhibited crystals of this form. Their work also suggests that the material filling in the voids was from dissolution along the stylolites.

As observed on the mesoscopic scale, the vein walls are wavy planar boundaries. The calcite veins crosscut the stylolites except in three cases which were used to calculate shortening of the unit. The veins range in width from about 0.005mm to over 5.0mm, with an average of approximately 0.05mm. Figure 24 shows a photograph comparing the two sizes of calcite veins. The continuity of the calcite veins on the microscopic level varies, but generally the wider the vein the more extensive it is. Most veins are continuous across the thin sections. The veins taper out in the same manner as the stylolites. Also as with the stylolites, there was no apparent spacing or zonal relations on this scale. The frequency of the calcite veins across a thin section varied widely, but extension calculations of the veins showed they represented the same overall amount of strain.

Several samples contained veins that showed more than one generation of fill, or a 'crack-seal' morphology(Ramsey, 1980). 'Crack-seal' deformation occurs where a fissure is opened by extension, and then material precipitates from fluids that fill in the void. The material is derived from pressure solution along the stylolites in the adjacent volume of rock. Continued stress causes the rock to fracture again, with the void again being filled by vein material. These two steps can be repeated any number of times. This process of repetition of the 'crack-seal' mechanism leads to development of a compound vein morphology, although to the naked eye the vein appears to be one solid infilling. Inclusions of matrix material occur in discrete zones that are parallel to the margins of the veins. These mark the positions of the vein walls in successive 'crack-seal' increments. These former walls identify repeated failure of the rock and infilling of the void. Figure 25 shows a photograph of a vein that has undergone crack-seal. The existence of this 'crack-seal' morphology in the veins establishes that they are definitely of an extensional origin.

The calcite veins as well as the calcite infillings of voids in the limestone show twinning in localized spots. Under tectonic stresses calcite will deform by mechanical twinning, commonly on the $\{01\bar{1}2\}$ planes, which is a deformation(gliding) twin(Deer, Howie, and Zussman, 1983). Under the microscope the twins appear as bands forming a diamond- shaped lattice in the calcite. The direction of maximum finite shortening of the unit is oriented roughly normal to the plane of the crystals containing the twins(Alvarez, Engelder, and Lowrie, 1976). The twin lamellae should be perpendicular to the stylolites(Nickelson,1973), and the ones observed in the thin sections generally were. Even though the presence of the twins in the calcite crystals indicates that localized ductile strain occurred within the limestones, their limited development means that the bulk flattening strain by this mechanism was minor.

STRAIN MEASUREMENTS

The majority of the strain measurements were done on the microscopic scale. These included estimating extensional strain by measuring vein widths, measuring shortening of the unit by calcite vein offsets along stylolites, and estimation of shortening by stylolite-truncated oncolites.

Extensional Strain.

The microscopic character of the calcite veins indicates that they produced extension of the Flagstaff Limestone. Based on the fact that the veins are oriented perpendicular to the hinge lines of the "S"-fold, extension must have occurred parallel to the hinge lines during formation of the fold. The amount of this extension during "S"-fold devel-

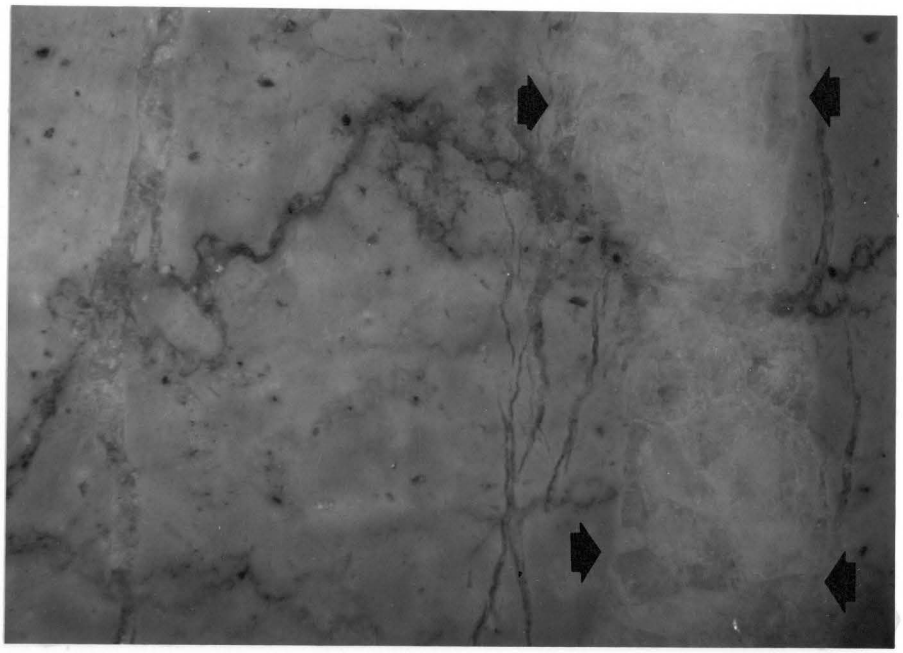

Figure 24. Photograph of adjacent large - and small-sized veins. The larger vein, marked by arrows, is an example of the veins theat were eliminated from the strain calculations. The smaller veins are of the typical size created by extension. Long axis of the photograph is 14 mm.

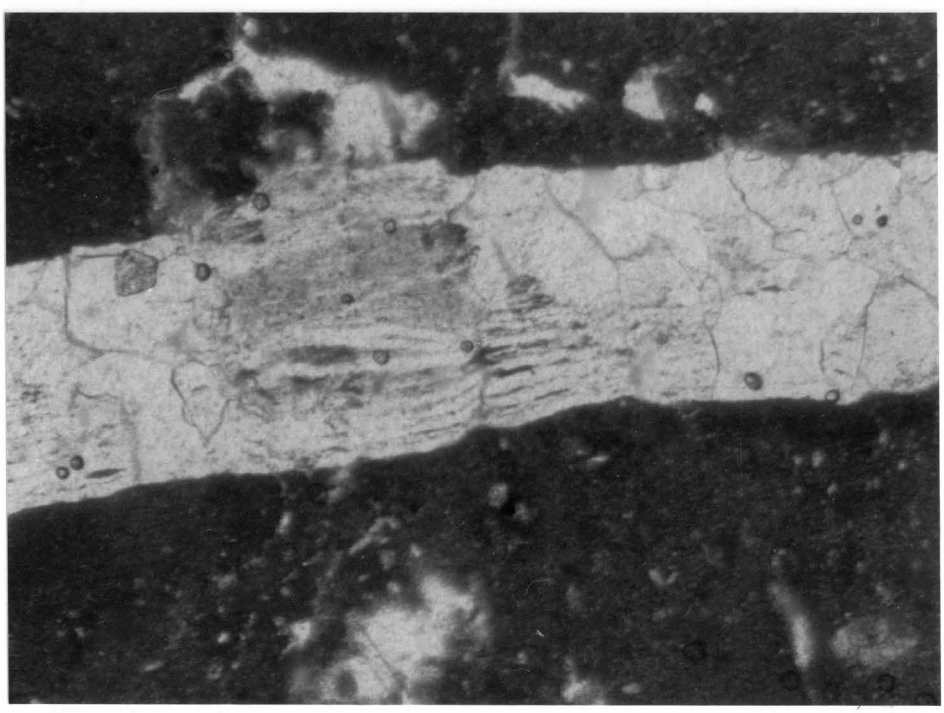

Figure 25. Photograph showing an example of a calcite vein that has undergone 'crack-seal' extension. The shadowy inclusions in the vein mark the former margins of the vein. Long axis of the picture is 2.1 mm.

opment was determined in slabs and thin sections cut perpendicular to both the calcite veins and the stylolites, in a plane containing the fold hinge line direction.

To estimate strain on both the hand samples and the thin sections, a summation of vein widths was taken across a traverse. Strain was calculated by the equation

$\Delta l/l$ = strain.

Strain is then multiplied by one hundred to determine a percent strain. Following is an example of how strain was calculated for thin section B4-3-B.

$\sum$ of vein widths = 0.695mm = Δl

l = traverse - Δl

= 25.00mm - 0.695mm

= 24.30mm

$\Delta l/l$ = (0.695mm)/(24.30mm)

=0.029

x100 = 2.9% strain.

Table 4 lists all of the strain calculations by percent and their location in the field. These include both hand samples and thin sections and are duely marked.

Table 4.

%strain	Station	Thin Sec.	Slabs	Pos. on fold
1.2	1	B2-1-A		lower hinge
1.5	1		B2-1-A	"
1.6	1		B2-1-B	"
1.8	1	B2-1-B-1		"
1.9	1		B2-1-B	"
2.0	1		B2-1-A	"
2.1	1		B2-1-A	"
2.2	1	B2-1-B-2		"
3.0	1		B2-1-B	"
3.8	1		B2-1-B	lower hinge
0.7	2	B2-2-A		steep limb
0.5	3	B4-3-B		west.limb
2.9	3	B4-3-A		"
3.3	3	B4-3-B		"
4.3	3	B4-3-D		"
0.7	5	B4-5-A-2		upper hinge
1.0	5	B4-5-A-1		"
1.6	5	B4-5-A-2		"

Table 4. Estimated percent extensional strain from calcite veins in hand samples and thin sections. They are identified by both sample and station.

In these calculations only the smaller veins discussed earlier were used. These averaged 0.05mm across. The sporadically developed larger veins were excluded, as they did not represent the typical extensional strain in the rock units as a whole. Strain including these larger veins was calculated to check this assumption. These strains were quite large and not within a reasonable range of the other estimates, whereas the strains calculated without the large veins were consistent. Therefore exclusion of the large veins is believed to be correct. The range of strain percents was 3.8%. The average was 2.0% extensional strain with a standard deviation of 1.2%. If the larger veins had been included, the average strain would be 7.7%, but the standard deviation would be 9.3%, a significant amount.

From Table 4 it can be seen that the largest strains occurred in the areas of the lower hinge and the shallowly westward-dipping limb. This is to be expected in the lower hinge because the hinge zone of the fold is the area of greatest strain during folding. The reason for this on the shallowly dipping limb relative to the rest of the "S"-fold may be because the limb suffered continued layer - parallel compression as opposed to the rest of the "S"-fold which underwent flexure, relieving it of this form of strain.

Shortening Strain

Bulk shortening of the limestone units was produced by pressure solution along the stylolites. This was evidenced by the presence of the well-developed interpenetrations of the 'teeth' across the stylolite surfaces, the truncations and offsets of rip-ups, oncolites, and calcite veins by stylolites, and the concentration of insoluble quartz and clay grains along the stylolites. The stylolites are systematically oriented perpendicular to bedding and parallel to the trend of the "S"-fold, indicating they formed due to layer-parallel compression which led to formation of the fold. The amount of bulk shortening strain accommodated by pressure solution along the stylolites was determined by two methods of strain measurement.

Calcite Vein Offset

The microscopic examination showed that the majority of the stylolites were cross-cut by the calcite veins, as was observed in the mesoscopic study. However, three calcite veins offset by stylolites were found. These intesections show that at least for a short period of time stylolites and calcite veins formed contemporaneously. It is believed that they were not found in greater abundance because of the limited sampling. These vein offsets were used to estimate the amount of shortening across a stylolite by the methods explained in Hancock and Atiya(1975). The conditions set by Hancock and Atiya are "that the generalized trend of the pseudo shear zone will be straight provided that the formerly continuous vein was straight, that pressure solution surfaces cutting it are parallel and evenly spaced, and the same width of material was removed at each surface". It was observed in the field that the planes of the calcite veins were generally straight,

and also that the stylolites were parallel and straight. Over the one meter traverse of the 'bundles', the stylolites were fairly evenly spaced.

Hancock and Atiya used the following equation to determine Wx, the width of the strip removed during pressure solution:

$Wx = a \tan\phi$ where

a = apparent slip along the pressure solution surface and

ϕ = the angle measured clockwise between the pressure solution surface and the vein.

Figure 26a shows a tracing of the offset intersection with a and ϕ drawn in for thin section B2-1-B-2. Figure 26b is a photograph illustrating a typical offset. Following is the shortening calculations for this section.

$\phi = 78°$

a = 0.0832mm

$Wx = (0.832mm)\tan 78°$

$= (0.832mm)(4.705)$

$= 0.391mm$, material removed.

Section B2-1-B-1 showed 0.396mm removed and section B4-3-D had 0.391mm removed. The difference between B2-1-B-2 and the other two thin sections may be attributed to the fact that its offset was dextral and the other two were sinistral. Dextral offsets, according to Hancock and Atiya, contain a true component of shear, which could account for the additional loss of material. Fine-grained insoluble minerals, concentrated by pressure solution, can form surfaces or zones of structural weakness, along which lateral motion(shear) can occur to relieve local stress(Wanless, 1979). Quartz grains found in many of the stylolites may have helped a minimal amount of shear to occur along the planes of the stylolites.

To get shortening on a larger scale and a percentage shortening, the above calculations were combined with the stylolite frequency data at Stations 1 and 3. The average frequencies were multiplied by the shortening over a stylolite(the two offsets at Station 1 were averaged for this purpose). This gave average shortening over a meter at both stations. Calculations were done as follows:

Avg. Frequency Station 1. = 7.26/m

Avg. Short./Stylolite Station 1. = 0.394mm

Shortening/m = 7.26/m (0.394mm)

= 2.86mm/m.

To determine the percent shortening the formula Wr/Wo from Hancock and Atiya was used, where Wr is width remaining and Wo is the original width. Wr was taken as 1000mm since shortening was calculated over a meter, and 1000mm + the calculated

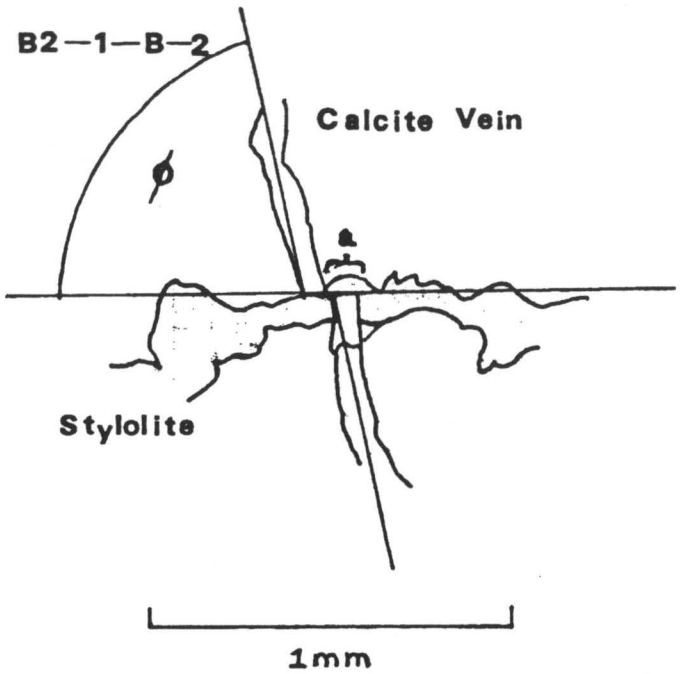

Figure 26a. This is an enlarged tracing of a sinistrally displaced vein used in calculating shortening. ø is the angle between the vein and the stylolite used in the equation from Hancock and Atiya (1975).

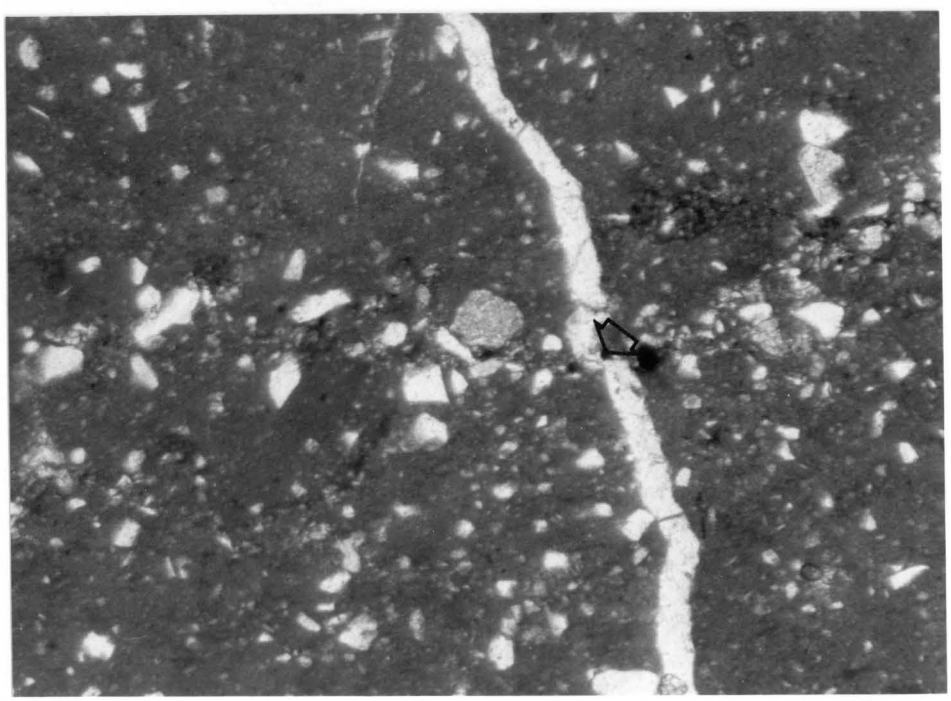

Figure 26b. Photograph of the offset calcite vein that was used in the example calcualtions for shortening strain. The long axis of the picture is 2.1 mm.

shortening was used for Wo. This produced results of 0.3% shortening strain at Station 1 and 0.4% shortening strain at Station 3.

The results of 0.3%and 0.4% shortening strain are similar to the lowest values of extensional strain. The data from the offsets represents a minimum amount of strain in the unit. These small values compared to the extensional strains suggest that shortening perpendicular to the fold hinges was exceeded by extension parallel to the hinges, or that there was a relative volume increase in the rock parallel to the fold hinge lines.

As discussed before, there is evidence for a minimal amount of shear having occurred. Also, the veins may not have formed until after the start of layer-parallel compression, and therefore do not represent the entire history of shortening. Nickelsen(1972) stated that irregular spacings of the stylolites would cause shortening to be limited to local solution because cleavage zones varied, and that these types of measurements were minimums.

Oncolite Truncations

Truncated oncolites were used as another method to determine shortening by pressure solution across the stylolites. The oncolites are common in the Flagstaff and North Horn Formations. These oncolites were particularly useful because they are spherical (Kulpanowski and Zawiskie, 1986). This was confirmed by axial ratio measurements of the oncolites. The ratios were approximately 1:1, meaning that the axes were the same length relative to each other in a specific oncolite and that that oncolite is round. The photograph in Figure 27a shows examples of truncated oncolites that were used for strain measurements. The clay material is missing along the stylolite due to thin section preparation. Figure 27b is a tracing of the photograph, depicting the positions of the stylolite and the oncolites it truncates.

To use the oncolites to determine shortening, they were traced and then a best-fit circle was made using a compass(see Figure 28.). The strikes of the stylolites were generally straight, indicating an equal amount of dissolution across them. An unequal amount of solution along a stylolite would have caused it to have an irregular surface or plane, not a straight line(Hancock and Atiya, 1984). This data was used to calculate a percentage shortening from $\Delta A/A$. It was assumed that strain was plane strain, meaning all of the shortening occurred in a plane perpendicular to the plane of the stylolite. This allowed the area of the tracings to be usedto estimate volume loss across a stylolite. The radius of the oncolites was taken from the best fit circle, and the original area of the oncolite was calculated using the equation $\prod r^2$ = Area of a circle.Then the missing area of the circle was estimated using the grid(as seen in Figure 28.) An example is given below of how strain was calculated for the oncolite in Figure 28.

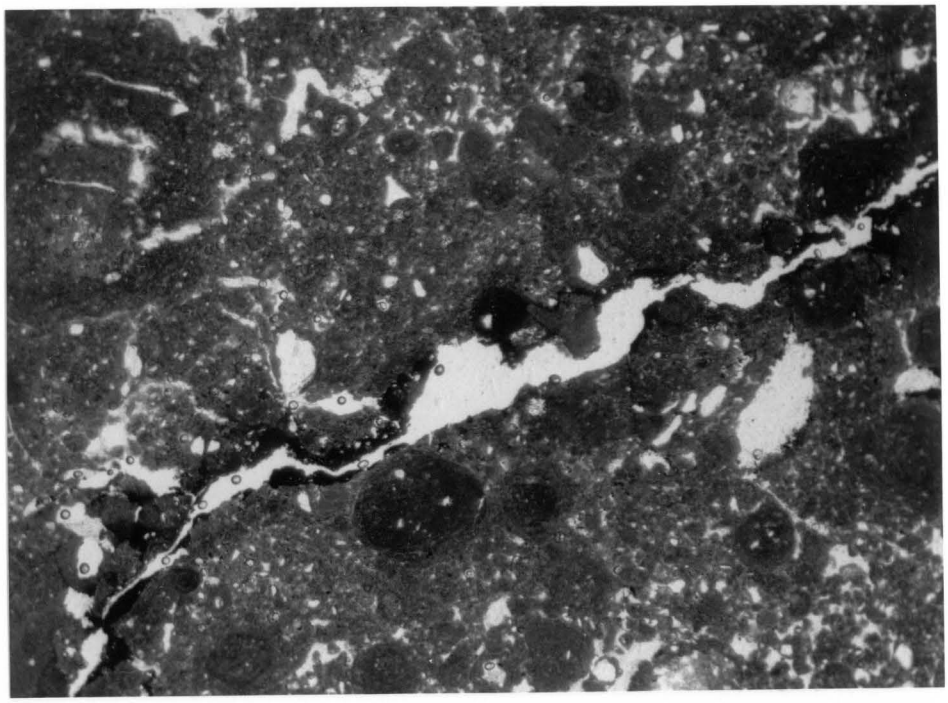

Figure 27a. Photograph showing spherical oncolites truncated by stylolites that were used for strain measurements. The light area along the stylolite represents voids formed when the clay material was removed during thin section preparation. The long axis of the picture is 2.1 mm.

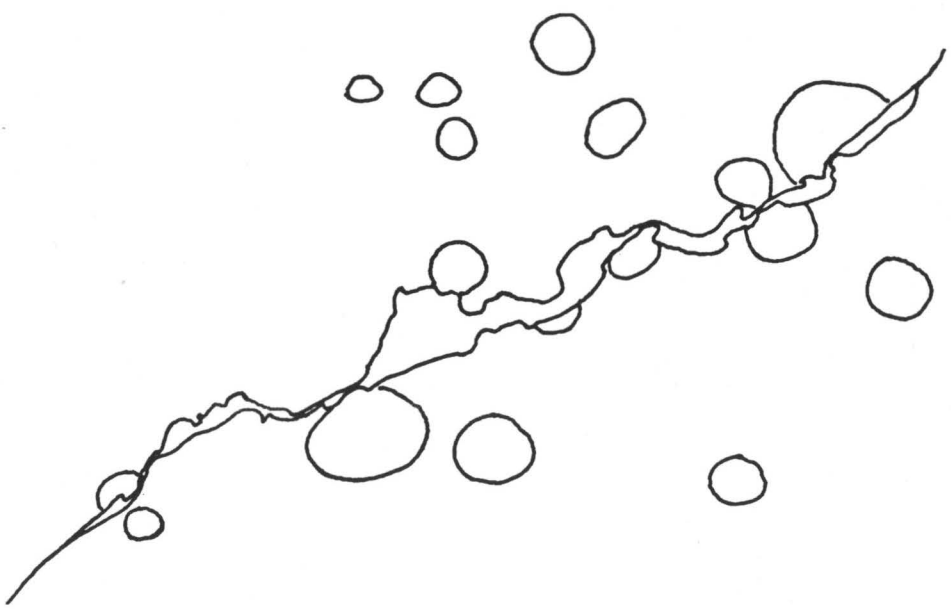

Figure 27b. Tracing of the photograph in 27a showing the position of the stylolite and the oncolites it truncates, as well as surrounding unaffected oncolites.

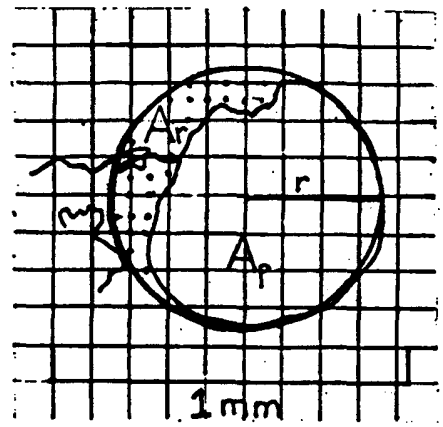

Figure 28. Enlargement of a truncated oncolit- tracing used in strain measurements across a stylolite. The best - fit circle was used to estimate the original volume of the oncolite.

$r = 0.364mm$

Area Original = A_0 $= \Pi(0.364mm)^2$

$= 0.416mm^2$

Area Removed = A_r $=0.0679mm^2$ (estimated from the grid)

Area Present = A_p $= A_o - A_r$

$= (0.416 - 0.0679)mm^2$

$= 0.348mm^2$

%Strain $= |(A_p - A_o) / A_o| \times 100$

$= |(0.348 - 0.416) / 0.416| \times 100$

$= 16.3\%$ strain

However, this is just the strain taken up by this particular oncolite. A bulk percent strain was calculated by determining the average percent strain recorded by oncolites in the two samples. These were 22.7% for sample B2-6-A-1 and 19.8% for sample B2-6-A-2. Then a percent of truncated oncolites versus total oncolites was calculated to find the amount of oncolites that actually took up strain (the non-truncated oncolites suffered no deformation). These were 17.3% and 8.89% respectively. These values were then multiplied by the average percent strain to yield the bulk shortening strain of the sample. Sample B2-6-A-1 suffered 3.93% shortening and sample B2-6-A-1 underwent 1.76% shortening strain. These two values include errors in area estimation compounded in the average percent strain for each sample, and in the calculation of the percent of truncated(strained) oncolites. The above calculations are on the conservative side.

When the results of the two shortening strain measurement methods are compared, it is seen that there is a sizable difference. The two values from the oncolite truncations are much closer to the average extensional strain of 2.0% calculated from the calcite vein

offsets. The average shortening strain was 1.6%. The difference between the two measurements may be because the calcite veins that the vein offset measurements are based on formed after the onset of stress, and therefore they are not representative of the entire strain history. The oncolites, on the other hand, were present during lithification of the rock and *do* represent all of the strain that occurred.

The results from the oncolite truncations are in much better agreement with the 2% average strain from the extensional measurements than the vein offset results are. Since the shortening strain and the extensional strain are close, relative volume change of the unit as indicated by the calcite vein offsets alone is not likely. This equality in strains is much more indicative of this non-penetrative deformation, where deformation was essentially volume constant with shortening across the planes of the stylolites compensated by extension across the calcite veins.

DISCUSSION

The "S"-fold along the eastern front of the Gunnison Plateau is not a major structure in size, but it is still important in the local tectonic history. At the site in Rock Canyon, a mesoscopic structural suite associated with the development of the "S"-fold was identified. This suite can be used to constrain models of formation for the fold.

At the field site in Rock Canyon the presence of stylolite cleavage planes was documented. They had consistent orientations striking north-northeast and were systematically subperpendicular to the bedding planes of the Flagstaff Formation, though they dipped steeply both to the northwest and southeast. Bedding planes were rotated about the line of strike to return them to a horizontal position. This gave all of the stylolites a near vertical orientation striking north northeast. Since all of the stylolites have this consistent orientation, they were formed prior to the folding of the unit and were rotated with the fold limbs. The orientations of the stylolites perpendicular to the bedding planes indicates they were created by a tectonic stress, as opposed to being horizontal and formed by an overburden stress(Wanless, 1979). This tectonic stress was layer-parallel compression, since the equal area projections show the stylolites formed in the same horizontal plane prior to folding. Limestone stylolitization is post-lithification pressure solution(Merino, et al, 1983). This means that the stylolites were a post-Early Eocene feature, since this was the end of deposition of the Flagstaff Formation. However, the stylolites are not indicative of a length of time for applied tectonic stress. Time for stylolite formation can range anywhere from 10 to 21,000 years in carbonates(Merino, et al, 1981). Nor are they indicative of how the mechanism worked. The "S"-fold could have been created by one steady period of stress or by several distinct episodes. Peter

Schwans(personal communication) believes his sedimentological studies in the region show the fold developed during several episodes of folding.

Several features in the rock suggest the stylolites in the Flagstaff Formation represent areas where pressure solution has occurred. Stylolitization occurs under compression of a unit leaving a residue of insoluble material to mark its presence(Merino, et al, 1981). Stylolites develop where dissolution increases the porosity of the rock along the plane of the stylolite. Continued stress causes physical collapse of the porous zones(Merino, et al, 1983). The presence of highly developed interpenetrating columnar teeth in the stylolites is highly indicative of pressure solution. Accummulation of insoluble quartz and clay grains along the stylolite surfaces is also evidence. Their concentrations are highly increased here as opposed to the rest of the unit. Calcite veins show offset along the planes of stylolites, indicating they have missing segments. Oncolites and 'rip-ups' in the rock also exhibit missing parts. These truncations are by removal of material across the stylolites.

Observations suggest that shortening in the Flagstaff Formation was accommodated by pressure solution on the stylolites. The consistent orientation of the stylolites perpendicular to bedding indicates that shortening due to layer-parallel compression was prior to initiation of folding. The stylolites strike parallel to the trends of the axial traces of the "S"-fold. This ties the formation of the two together in the same compressional event. The lack of oriented long axes in the 'rip-ups' and any shape changes in the spherical oncolites shows that there was little or no penetrative ductile strain of the bedding layers. Deformation occurred only along the stylolite planes, and shortening was due solely to pressure solution along the stylolites. The lack of well-developed mechanical twinning in the calcite crystals in the limestone supports this conclusion.

The structural suite at the site in Rock Canyon was also shown to contain calcite veins. The planes of these veins strike west-northwest and are perpendicular to the stylolites as well as the hinge lines of the "S"-fold. This systematic geometric orientation relative to the stylolites and hinge lines indicates that the calcite veins are contemporaneous with these structural features. This is supported by the mutual crosscutting relations of the stylolites and veins, though the majority of the cases were veins cutting stylolites. It was not possible to use equal area projection rotations to determine if the veins were pre- or post-folding because they are perpendicular to the hinge lines. Vein development may have continued after layer-parallel shortening and after stylolite formation ceased, possibly indicating the onset of folding. They would then represent a different method of relieving stress.

The morphology of the calcite veins consists of blocky calcite crystals with their long axes perpendicular to the walls of the veins. This indicates an extensional origin for the veins. Extension was perpendicular to the vein margins. The work Mullenax and

Gray (1984) did on stylolites and veins in folds also showed extensional veins with similar blocky calcite crystals. The compound veins and inclusion trains found on many of the thin sections supports an extensional origin by 'crack-seal' deformation. This is repeated cycles of sealing of extension fractures by precipitation of vein material. Observations indicate that the calcite veins accommodated extension parallel to the direction of the "S"-fold hinge lines.

Both extensional and shortening strains were calculated. The values of strains associated with the development of the mesoscopic structural suite were small. Extensional strain parallel to the direction of the "S"-fold hinge line directions averaged 2.0%. Shortening strain across stylolites was estimated at 0.35% for calcite vein offsets. However, these offsets may only record part of the shortening if the affected veins developed late in the progressive deformation of the area. A large number of measurements would be needed to test this. The average calculated shortening strain from the truncated oncolites was 2.84%. This is an approximate match to the extensional strain. This is suggestive of a volume constant bulk deformation of the rock mass. This means that the material dissolved by pressure solution along the stylolites diffused through the local rock volume and was reprecipitated in the opening extensional fissures. Mullenax and Gray(1984) found this to be the typical deformation style at upper crustal levels in folds they studied with similar structural suites. Ramsay(1980) defined his 'crack-seal' mechanism as operating in this manner, and Burger and Thompson(1970) described similar results from cleavage planes of the Carmichael Peak Anticline in Montana.

The interpenetrative columnar teeth of the stylolites are perpendicular to the planes of the stylolites. Because these points of interpenetration represent sites of maximum pressure solution, the trends of the teeth are parallel to the maximum principal compressive stress direction(Alvarez, et al, 1976). The extensional veins, such as those created by 'crack-seal', are examples of hydraulic fracture of the rock mass due to elevated pore fluid pressures(Ramsay, 1980). Figure 29 shows a sketch of the greatest (σ_1)and least (σ_3) principal stress directions, and the orientation of the structural suite that formed in response to these directions. This is based on the assumption that the planes of the calcite veins are oriented perpendicular to the least(σ_3)principal compressive stress, and contain the greatest(σ_1) and intermediate(σ_2) principal compressive stresses within their planes. The veins open up parallel to the least principal compression direction. These two features can be used to determine the three stress orientations that created the "S"-fold(Figure 29). The average trend of the stylolite teeth from the lower hinge and the western limb indicate that the greatest principal compressive stress was oriented at 127, or approximately northwest-southeast. In the same manner the average calcite extension vein showed a least principal compressive stress oriented at 015, or north northeast-south southwest. The intermediate stress was vertical and perpendicular to both of the other

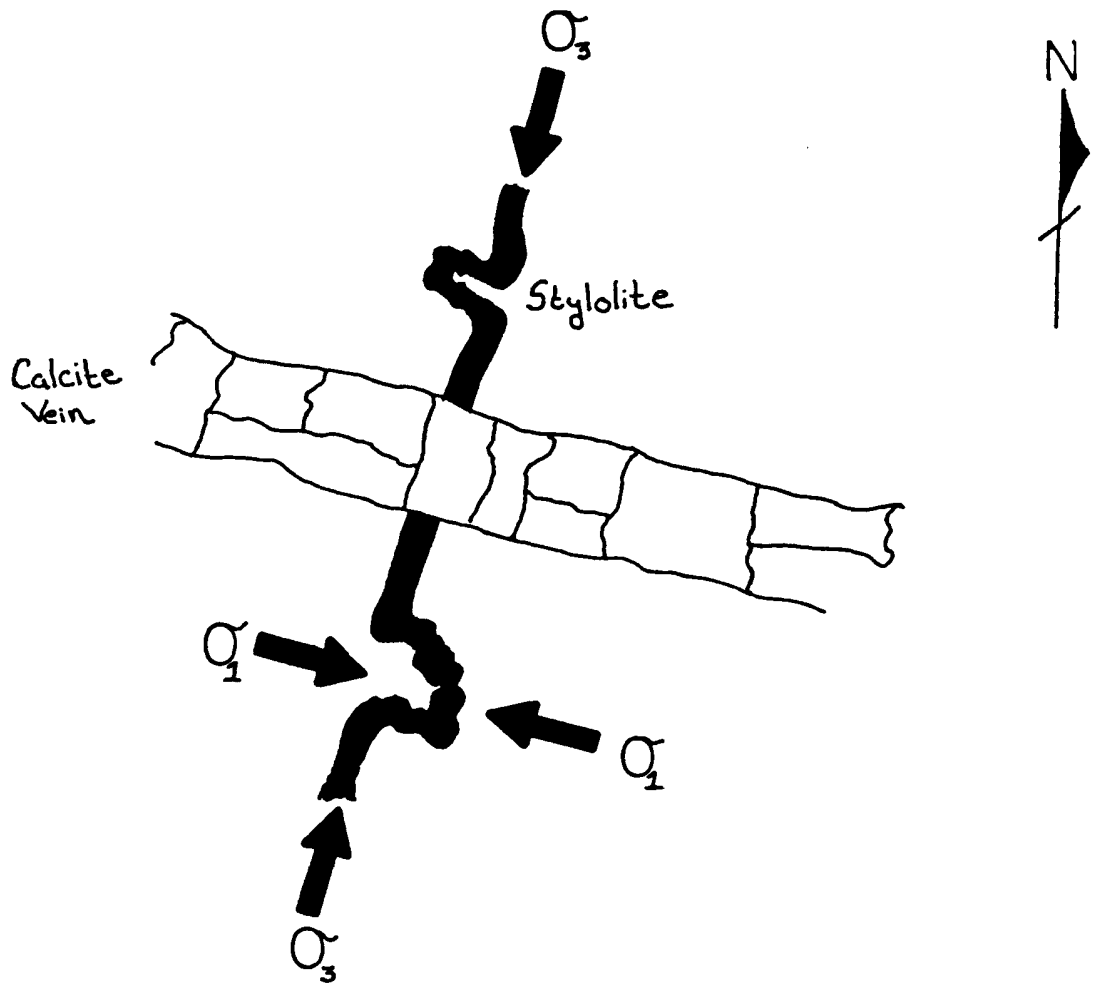

Figure 29. Greatest (σ_1) and least (σ_3) principal compressive stress orientations that formed the stylolites and calcite veins. The greatest principal stress is oriented west-northwest - east-southeast.

stress directions. It can be seen that the greatest and least principal compressive stresses are not mutually perpendicular as they should be, though they are relatively close. The average strike of the stylolites, which is perpendicular to the maximum stress direction or parallel to the least, is 019. This is more consistent with the results from the calcite extension veins. The average trend of the stylolite teeth on the western limb was 095, which by itself would orient the maximum compressive stress in better agreement and much closer to perpendicular to $_3$ determined from the veins. This indicates that the data from the teeth in the lower hinge (trend 159) is inaccurate or has been affected by an unconsidered factor. Possible errors could lie in the measurements, since the size of the teeth made this very difficult or local inhomogeneities in the limestone could have affected pressure solution formation of the teeth in such a way as they did not form perpendicular to the plane of the stylolites.

Based on the fact that the stylolite teeth are perpendicular to the planes of the stylolites, and therefore the axial traces of the "S"-fold, the greatest principal compressive stress direction was perpendicular to the fold hinge lines. This shows the fold was buckled by this maximum compressive stress direction. The least principal compressive stress direction was parallel to the hinge lines, and extension occurred in this direction. This data is consistent with the stress orientations that caused the Sevier folding and thrusting that created the Gunnison Plateau(Villien and Kligfield, 1986 and Spieker, 1946).

Implications of Results for "S"-fold Development

The investigation of the structural suite at Rock Canyon when related to fold development indicates that this monocline or asymmetric flexure formed in response to a west northwest to east southeast compressional stress. Initial layer-parallel compression caused shortening of the units by pressure solution along the planes of the stylolites. Initiation and amplification of the "S"-fold followed this. Because stylolitization is a post-lithification process(Merino, et al, 1983), the fold must be related to tectonic stresses that affected the region after lithification of the Flagstaff Limestone, and are therefore post-Early Eocene in age.

Witkind(1982) believes these stresses were caused by salt diapirism in the Jurassic Arapien Shale. He interprets the structure of the eastern flank of the Gunnison Plateau, including the "S"-fold, as the remnants of the eroded flank of an anticlinal fan fold created by the rise of a diapir. Witkind's diapiric model(see Figure 4b) implies an oblique outward 'push' of sedimentary strata by the rising diapir creating the fold. This would produce compressional stresses at an oblique angle to sedimentary layering, but the stylolites documented in this study show that fold development was associated with *layer-parallel* compression. This result is not consistent with Witkind's salt diapir model.

Another inconsistency with Witkind's model is that his model implies that the Jurassic units such as the Twist Gulch Member should have been strongly deformed by the rise of the diapirs, and then further disturbed by collapse into the voids created by the dissolution of the salts. It was observed in the Rock Canyon region that the Twist Gulch Member was tilted, presumably due to folding, prior to development of the "S"-fold. The Twist Gulch displayed bedding planes that had maintained their integrity, and there was no evidence for the strong disruption and dissolution Witkind's model predicts. There are evaporites present in Central Utah, but they are *not* tectonically significant in this region.

Weiss(1982) attributes development of the "S"-fold to upward and westward motion of the Sanpete Valley Antiform to the east of the Gunnison Plateau. Weiss believes the Jurassic strata were "jammed" against the North Horn and overlying Flagstaff strata,

forcing them to fold in an asymmetric fashion. He appears to favor Witkind's diapiric model as the driving force for the antiform. Upward and westward movement by the antiform is inconsistent with the evidence for layer-parallel compression previously discussed. The Sanpete Valley Antiform is probably responsible for thinning the North Horn along its flanks, but folding has already been established as post-Early Eocene, and the antiform was inactive by this time(Weiss, 1982).

In the regional cross sections presented by Villien and Kligfield(1986), the Gunnison Plateau is bounded on the eastern flank by the west-vergent, eastward-dipping backthrusts of the Wasatch System from the Wasatch Plateau westward across the Sanpete Valley to the Gunnison Plateau. Figure 30 shows a cross section of the Gunnison - Sanpete Valley - Wasatch region, showing the backthrusts riding on top of the Wasatch Thrust System and up the face of the Gunnison Plateau. These backthrusts developed during the Late Paleocene thrusting phase. Villien and Kligfield believe that all major tectonic activity had ended by this time, and that folding had occurred prior to deposition of the Flagstaff Formation. Schwans(1987) agrees with this completion of folding by the Late Paleocene, buut points out that dating of the units varied by locality and that a narrow time frame could not be placed on the "S"-fold. However, as discussed earlier in this paper, the presence of the stylolites in the Flagstaff Limestone indicates folding did not commence until post-Early Eocene. Because Villien and Kligfield's thrust regime developed in response to an east-west regional compression, this model could be consistent with development of the "S"-fold if this compression continued into the Eocene.

The following model of fold development is derived from the Villien and Kligfield backthrusting geometry shown in Figure 30. The sketches in Figure 31 depict the four major stages of the model for development of the "S"-fold.

The first stage of fold development was layer-parallel compression producing shortening in the Flagstaff Formation. The west northwest directed compressional stress indicated by the stylolite teeth created shortening. Figure 31a shows that this was prior to folding.

Stage 2 was continued east-west compression causing inhomogenous distortion of the units. This initiated slip along the bedding planes of the eastward-dipping Jurassic Twist Gulch Member strata, representing local west-vergent backthrusts. Reverse motion along the Twist Gulch bedding planes caused the North Horn and Flagstaff Formations above the unconformity to flex or 'arch' upwards forming the "S"-fold as seen in Figure 31b. The lack of visible displacement of the Twist Gulch beds supports movement parallel to the bedding planes. The fold marks the position where the backthrusts slid up along the face of the plateau.

The third stage, the timing of peak amplification of the fold, was the most difficult aspect to determine. The absence of the Colton and the Green River Formations at the

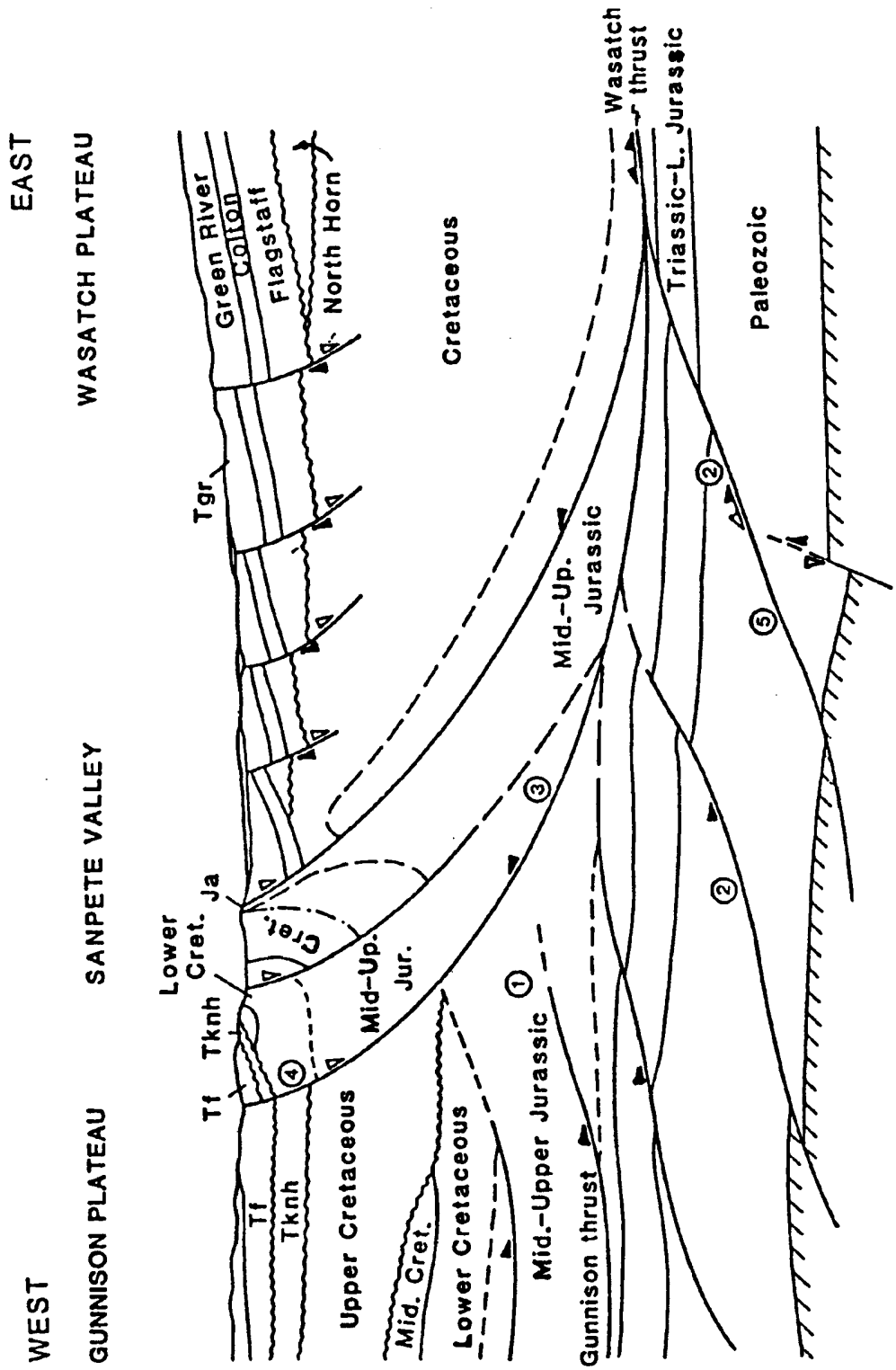

Figure 30. Cross section from the Gunnison Plateau to the Wasatch Plateau. It shows the backthrust riding on top of the Wasatch and Gunnison Thrusts and up the face of the Gunnison Plateau, folding the units above. The backthrust has distorted the unconformities and thicknesses of the units in appearance. The backthrust may be listric at depth. Black arrowa represent initial movement along the faults. White arrows represent onset of normal movement due to extension of the valley(Villien and Kligfield, 1986).

site in Rock Canyon due to erosion only establishes a post-Early Eocene completion of the "S"-fold. It is noy known whether these units were affected by folding(see Figure 31c). Only a time frame of post-Early Eocene to Middle Miocene(approximate commencement of Basin and Range extension) can definitely be placed on the fold. However, to the west of the study site, on top of the Gunnison Plateau, the Colton and Green River lie conformably upon the Flagstaff, and just to the south in the Sanpete Valley the Colton and Green River are involved in anticlinal structures. Compression from backthrusting could have caused these structures, dragging the strata above the thrust beds along like a carpet. No compressive structures are superimposed on either the "S"-fold or these anticlines, indicating that they could be the last compressive features of the region. If the "S"-fold and the anticlines were created by the same compression, this would put an age on the completion of folding in the Late Oligocene - Early Miocene.

The fourth and final stage of the model is the onset of Basin and Range extension pictured in Figure 31d. This initiated normal faulting as the Sanpete Valley extended, and possible normal movement along the backthrusts(Weiss, 1982). Faults did truncate the "S"-fold and are responsible for blocks of the fold dropping down to the east of the study site.

FIGURE 31 a-d (see following page). These four sketches represent the evolution of the "S"-fold in Rock Canyon.
a) Pre-folding position of beds during layer-parallel compression and formation of the stylolites, post-Early Eocene.
b) Commencement of buckling of the fold as the backthrust Twist Gulch beds force the overlying units to flex.
c) Completion of amplification of the "S"-fold, anywhere from the post-Early Eocene to Middle Miocene.
d) Normal movement along faults causing collapse of the "S"-fold due to Basin and Range extension widening the Sanpete Valley.

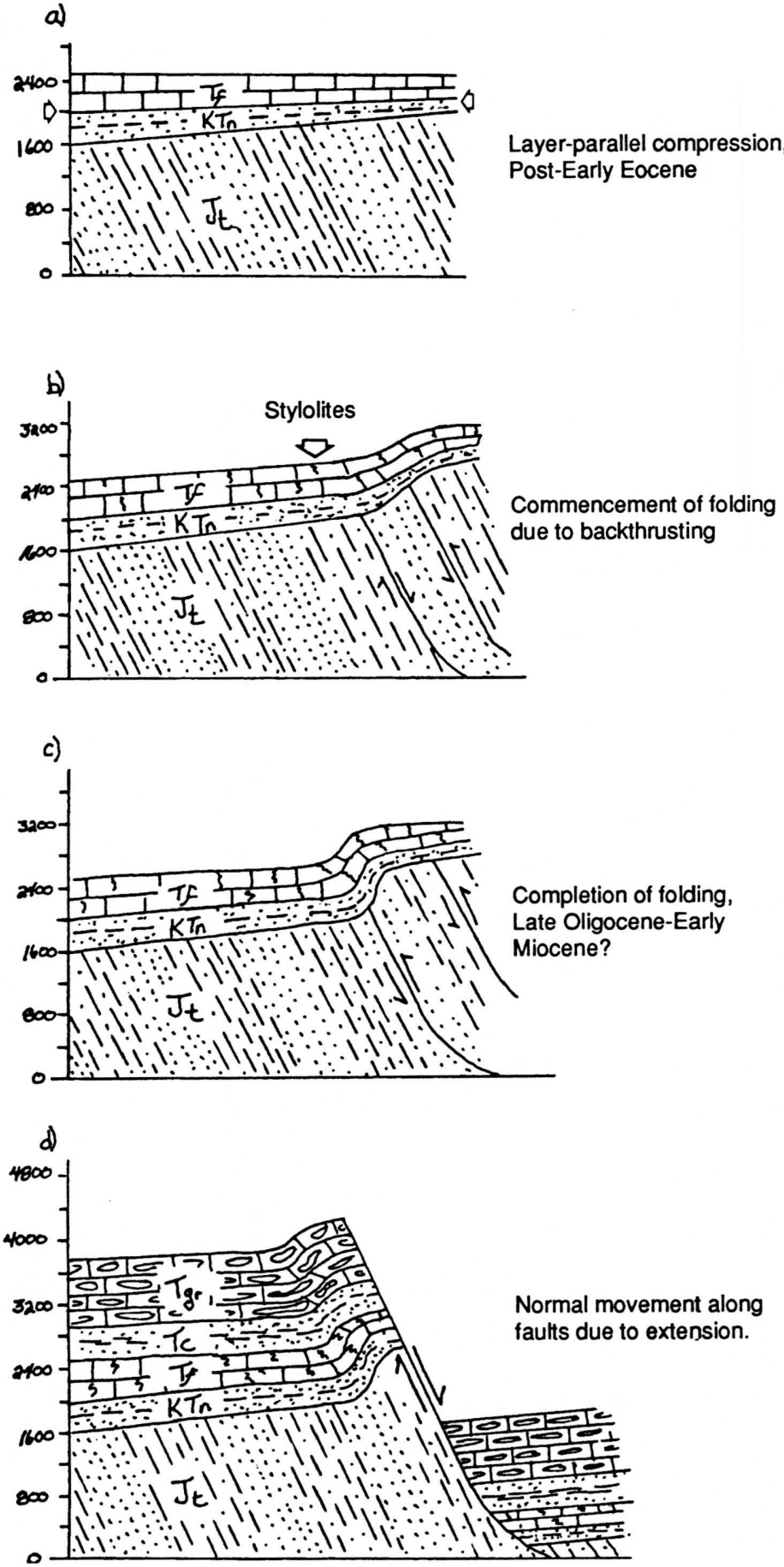
a)
2400
1600
800
0
Tf
KTn
Jt
Layer-parallel compression,
Post-Early Eocene
b)
Stylolites
3200
2400
1600
800
0
Tf
KTn
Jt
Commencement of folding
due to backthrusting
c)
3200
2400
1600
800
0
Tf
KTn
Jt
Completion of folding,
Late Oligocene-Early
Miocene?
d)
4800
4000
3200
2400
1600
800
0
Tgr
Tc
Tf
KTn
Jt
Normal movement along
faults due to extension.
Thickness(feet)

CONCLUSIONS

The "S"-fold in Rock Canyon along the eastern flank of the Gunnison Plateau was formed by backthrusting of Twist Gulch Member beds, causing flexure in the overlying units. Based on the examination of stylolites and calcite veins, folding was caused by layer-parallel compression in a west northwest-east southeast direction in the post-Early Eocene. Strain measurements showed that deformation in the Flagstaff Limestone was non-penetrative and that bulk shortening and extension occurred only along the stylolites and calcite veins. Shortening ranged from 0.3% to 3.93% and extension from 0.5% to 4.3 %. Strain was greatest in the lower hinge and western limb. Completion of folding could only be definitely framed from post-Early Eocene to Middle Miocene due to erosion of the upper sedimentary units at the site.

REFERENCE

Alvarez, Walter, Engelder, Terry, and Lowrie, William, 1976, Formation of Spaced Cleavage and Folds in Brittle Limestone by dissolution: Geology, v.4, p.698 - 701.

Bombolakis, E. G., and Delphia, John G., 1986, Some Kinematics, Mechanics, and Dynamics in the Development of a Foreland Fold - and - Thrust Belt: EOS Transactions, American Geophysical Union, v.67, #4, T41C - 15 1151H.

Burger, H. Robert III, and Thompson, Margeret D., 1970, Fracture Analysis of the Carmichael Peak Anticline, Madison County, Montana: Geological Society of America Bulletin, v.81, p.1831 - 1836.

Deer, Howie, and Zussman, An Introduction to the Rock Forming Minerals, Longman House Limited, 1983, p. 476 - 485.

Dunnet, D., 1969, A Technique of Finite Strain Analysis Using Elliptical Particles, Tectonophysics, v.7, p. 117 - 136.

Hancock, P.L., and Atiya, M.S., 1975, The Development of En-e´chelon Vein Segments by the Pressure Solution of Formerly Continuous Veins: Proceedings of the Geo logical Association, v.86, #3, p.281 - 286.

Jefferson, William S., 1983, Provenance Relations Between Synorgenic Indianola Group and Late Cretaceous Thrusting (Sevier), Cedar Hills, Central Utah: 36th Annual Meeting Rocky Mountain Section, Geological Society of America: Abstract with Programs, May 2-4, 1983, University of Utah, Salt Lake City, Utah, p. 377.

Kligfield, Roy, 1982, Strain Patterns of Extensional Origin: 95th Annual Meeting, Geological Society of America: Abstract with Programs, August 1982, New Or leans, Louisiana, p.532.

Kulpanowskie, S.E., and Zawiskie, J.M., 1986, Fluvial and Marginal Lacustrine Algal Facies: North Horn and Flagstaff Formations, U. Cretaceous to L. Eocene, Gunni son Plateau, Central Utah: North Central Section, Geological Society of America: Abstract with Programs, March 1986, Kent State University, Kent, Ohio, p.313 - 314.

Lawton, T.F., and Mayer, Larry, 1982, Thrust Load Induced Basin Subsidence and Sedimentation in the Utah Foreland: Temporal Constraint on the Upper Cretaceous Sevier Orogeny: 95th Annual Meeting, Geological Society of America: Abstract with Programs, August 1982, New Orleans, Louisiana, p.542.

McClay, Ken, The Mapping of Geologic Structures, Ch.7 Joints, Veins, and Stylolites, Open University Press, 1987, p.116 - 125.

Mackintosh, David M., 1967, Quartz - Carbonate Veining and Deformation in Namurian Turbidite Sandstones of the Crackington Measures, North Cornwall: Geol. Maga zine, v.104, #1, p.75 - 85.

Meike, Annemarie, 1983, Microstructures of Stylolites in Limestone: 96th Annual Meeting, Geological Society of America: Abstract with Programs, p.642.

Merino, Enrique, Ortoleva, Peter, and Strickholm, Peter, 1981, Stylolites in Sedimentary Rocks: A Pressure Solution Kinetic Theory for Their Generation and Regular Spacing: EOS Transactions, American Geophysical Union, v.62, #27-52, p.1056.

Merino, Enrique, Ortoleva, Peter, and Strickholm, Peter, 1983, Generation of Evenly - Spaced Pressure Solution Seams During (Late) Diagenesis: A Kinetic Theory: Contributions to Mineralogy and Petrology, v.82, #4, p.360 -370.

Mullenax, A. Craig, and Gray, David R., 1984, Interaction of Bed-parallel Stylolites and Extension Veins in Boudinage: Journal of Structural Geology, v.6, #1-2, p.63 - 71.

Nickelsen, Richard P., 1972, Attributes of Rock Cleavage in Some Mudstones and Limestones of the Valley and Ridge Province, Pennsylvania: Pennsylvania Academy Science Proc., v.46, p.107 - 112.

Picard, M. Dane, 1979, Petrology of Arapien Shale and Original Evaporite, Central Utah: 92nd Annual Meeting, Geological Society of America: Abstract with Programs, v.11, August 1979, p.495.

Plessman, W., 1972, Horizontal - Stylolithen im Franzosisch - Scweizerischen Tafel und Faltenjura und ihre Einpassung in den Regionalen Rahnen: Geolog. Runschau, v.61, p.332 - 347.

Ramsay, John G., 1980, The Crack-Seal Mechanism of Rock Deformation: Nature, v.284, #5752, p.135 - 139.

Scwans, Peter, 1987, Sedimentological Effects of the Tectonic Transition From Fold-Thrust Deformation to Thrust-Cored Uplift, Proximal Sevier Foreland (Six Mile - Price River North Horn Interval), Campanian - Paleogene of Utah: Geological Society of America: Abstract with Programs, v.19, #5, p.332.

Spieker, E.M., 1946, Late Mesozoic and Early Cenozoic History of Central Utah: U.S. Geol. Survey Prof. Paper 205-D, p.i - iv and 117 - 161.

Spieker, E.M., 1949, Sedimentary Facies and Associated Diastrophism in the Upper Cretaceous of Central and Eastern Utah, Sedimentary Facies in Geologic History: Geological Society of America Memoirs 39, p.55 - 82.

Stanley, K.O., and Collinson, James W., 1979, Depositional History of Paleocene - Lower Eocene Flagstaff Limestone and Coeval Rocks, Central Utah: Am. Assoc. of

Pet. Geol. Bulletin, v.63, #3, p.511, 323.

Villien, A., and Kligfield, R.M., 1986, Thrusting and Synorogenic Sedimentation in Central Utah: in AAPG Memoir 41 Paleotectonics & Sedimentation (in Rocky Mountain Region, United States), Edited by James A. Petersen, The American Association of Petroleum Geologists, Tulsa, Oklahoma, U.S.A., 1986, p.281 - 307.

Wanless, Harold Rogers, 1979, Limestone Response to Stress: Pressure Solution and Dolomitization: Journal of Sed. Petrol., v.49, #2, p.437 - 462.

Weiss, Malcolm P., 1982, Structural Variety on East Front of the Gunnison Plateau, Central Utah: Utah Geol. Assoc. Publication, v.10, p.49 - 63.

Weiss, Malcolm P., 1983, Gunnison Plateau: Passive or Active Block?: 36th Annual Meeting Rocky Mountain Section, Geological Society of America: Abstract with Programs, May 2-4, 1983, University of Utah, Salt Lake City, Utah, p.372.

Witkind, Irving J., 1982, Salt Diapirism in Central Utah: Utah Geol. Assoc. Publication, v.10, p.13 - 30.